

Search for the dark photon in $B^0 \rightarrow A'A'$, $A' \rightarrow e^+e^-, \mu^+\mu^-,$ and $\pi^+\pi^-$ decays at Belle

The Belle Collaboration



S.-H. Park,⁹⁵ Y.-J. Kwon,⁹⁵ I. Adachi,^{17,13} H. Aihara,⁸⁸ S. Al Said,^{81,36} D. M. Asner,³
H. Atmacan,⁷ T. Aushev,¹⁹ R. Ayad,⁸¹ V. Babu,⁸ P. Behera,²⁵ J. Bennett,⁵²
M. Bessner,¹⁶ V. Bhardwaj,²² B. Bhuyan,²³ T. Bilka,⁵ J. Biswal,³³ G. Bonvicini,⁹³
A. Bozek,⁶² M. Bračko,^{49,33} T. E. Browder,¹⁶ M. Campajola,^{30,57} L. Cao,²
D. Červenkov,⁵ M.-C. Chang,¹⁰ P. Chang,⁶¹ A. Chen,⁵⁹ B. G. Cheon,¹⁵ K. Chilikin,⁴³
H. E. Cho,¹⁵ K. Cho,³⁸ S.-J. Cho,⁹⁵ S.-K. Choi,¹⁴ Y. Choi,⁷⁹ S. Choudhury,²⁴
D. Cinabro,⁹³ S. Cunliffe,⁸ S. Das,⁴⁸ N. Dash,²⁵ G. De Nardo,^{30,57} F. Di Capua,^{30,57}
J. Dingfelder,² Z. Doležal,⁵ T. V. Dong,¹¹ S. Eidelman,^{4,66,43} D. Epifanov,^{4,66}
D. Ferlewicz,⁵¹ B. G. Fulsom,⁶⁸ R. Garg,⁶⁹ V. Gaur,⁹² A. Garmash,^{4,66} A. Giri,²⁴
P. Goldenzweig,³⁴ Y. Guan,⁷ K. Gudkova,^{4,66} C. Hadjivasiliou,⁶⁸ T. Hara,^{17,13}
O. Hartbrich,¹⁶ K. Hayasaka,⁶⁴ H. Hayashii,⁵⁸ M. T. Hedges,¹⁶
M. Hernandez Villanueva,⁵² W.-S. Hou,⁶¹ C.-L. Hsu,⁸⁰ K. Huang,⁶¹ T. Iijima,^{56,55}
K. Inami,⁵⁵ G. Inguglia,²⁹ A. Ishikawa,^{17,13} R. Itoh,^{17,13} M. Iwasaki,⁶⁷ Y. Iwasaki,¹⁷
W. W. Jacobs,²⁶ I. Jaegle,⁹ E.-J. Jang,¹⁴ H. B. Jeon,⁴¹ S. Jia,¹¹ Y. Jin,⁸⁸
C. W. Joo,³⁵ K. K. Joo,⁶ K. H. Kang,⁴¹ G. Karyan,⁸ T. Kawasaki,³⁷ C. Kiesling,⁵⁰
D. Y. Kim,⁷⁸ K.-H. Kim,⁹⁵ S. H. Kim,⁷⁵ Y.-K. Kim,⁹⁵ K. Kinoshita,⁷ P. Kodys,⁵
T. Konno,³⁷ S. Korpar,^{49,33} D. Kotchetkov,¹⁶ P. Krizan,^{45,33} R. Kroeger,⁵²
P. Krokovny,^{4,66} T. Kuhr,⁴⁶ M. Kumar,⁴⁸ K. Kumara,⁹³ K. Lalwani,⁴⁸ I. S. Lee,¹⁵
S. C. Lee,⁴¹ C. H. Li,⁴⁴ J. Li,⁴¹ L. K. Li,⁷ Y. B. Li,⁷⁰ L. Li Gioi,⁵⁰ J. Libby,²⁵
K. Lieret,⁴⁶ Z. Liptak,^{16,†} D. Liventsev,^{93,17} T. Luo,¹¹ J. MacNaughton,⁵³
C. MacQueen,⁵¹ M. Masuda,^{87,72} T. Matsuda,⁵³ D. Matvienko,^{4,66,43} M. Merola,^{30,57}
F. Metzner,³⁴ K. Miyabayashi,⁵⁸ R. Mizuk,^{43,19} G. B. Mohanty,⁸² S. Mohanty,^{82,91}
T. Mori,⁵⁵ H.-G. Moser,⁵⁰ M. Mrvar,²⁹ R. Mussa,³¹ M. Nakao,^{17,13} Z. Natkaniec,⁶²
A. Natochii,¹⁶ L. Nayak,²⁴ M. Nayak,⁸⁴ M. Niiyama,⁴⁰ N. K. Nisar,³ S. Nishida,^{17,13}
S. Ogawa,⁸⁵ H. Ono,^{63,64} Y. Onuki,⁸⁸ P. Oskin,⁴³ P. Pakhlov,^{43,54} G. Pakhlova,^{19,43}

[†]now at Hiroshima University

S. Pardi,³⁰ C. W. Park,⁷⁹ H. Park,⁴¹ S. Patra,²² S. Paul,^{83,50} T. K. Pedlar,⁴⁷
 R. Pestotnik,³³ L. E. Piilonen,⁹² T. Podobnik,^{45,33} V. Popov,¹⁹ E. Prencipe,²⁰
 M. T. Prim,³⁴ M. Ritter,⁴⁶ M. Röhrken,⁸ A. Rostomyan,⁸ N. Rout,²⁵ G. Russo,⁵⁷
 Y. Sakai,^{17,13} S. Sandilya,²⁴ A. Sangal,⁷ L. Santelj,^{45,33} T. Sanuki,⁸⁶ V. Savinov,⁷¹
 G. Schnell,^{1,21} J. Schueler,¹⁶ C. Schwanda,²⁹ Y. Seino,⁶⁴ K. Senyo,⁹⁴ M. E. Sevier,⁵¹
 M. Shapkin,²⁸ C. Sharma,⁴⁸ C. P. Shen,¹¹ J.-G. Shiu,⁶¹ A. Sokolov,²⁸ E. Solovieva,⁴³
 S. Stanić,⁶⁵ M. Starić,³³ Z. S. Stottler,⁹² J. F. Strube,⁶⁸ M. Sumihama,¹²
 K. Sumisawa,^{17,13} T. Sumiyoshi,⁹⁰ W. Sutcliffe,² M. Takizawa,^{76,18,73} K. Tanida,³²
 F. Tenchini,⁸ M. Uchida,⁸⁹ T. Ugllov,^{43,19} Y. Unno,¹⁵ S. Uno,^{17,13} P. Urquijo,⁵¹
 S. E. Vahsen,¹⁶ R. Van Tonder,² G. Varner,¹⁶ K. E. Varvell,⁸⁰ A. Vinokurova,^{4,66}
 V. Vorobyev,^{4,66,43} E. Waheed,¹⁷ C. H. Wang,⁶⁰ E. Wang,⁷¹ M.-Z. Wang,⁶¹
 P. Wang,²⁷ M. Watanabe,⁶⁴ S. Watanuki,⁴² S. Wehle,⁸ E. Won,³⁹ X. Xu,⁷⁷
 B. D. Yabsley,⁸⁰ W. Yan,⁷⁴ S. B. Yang,³⁹ H. Ye,⁸ J. Yelton,⁹ J. H. Yin,³⁹ Y. Yusa,⁶⁴
 Z. P. Zhang,⁷⁴ V. Zhilich,^{4,66} V. Zhukova,⁴³ V. Zhulanov,^{4,66}

¹University of the Basque Country UPV/EHU, 48080 Bilbao, Spain

²University of Bonn, 53115 Bonn, Germany

³Brookhaven National Laboratory, Upton, New York 11973, USA

⁴Budker Institute of Nuclear Physics SB RAS, Novosibirsk 630090, Russian Federation

⁵Faculty of Mathematics and Physics, Charles University, 121 16 Prague, The Czech Republic

⁶Chonnam National University, Gwangju 61186, South Korea

⁷University of Cincinnati, Cincinnati, OH 45221, USA

⁸Deutsches Elektronen-Synchrotron, 22607 Hamburg, Germany

⁹University of Florida, Gainesville, FL 32611, USA

¹⁰Department of Physics, Fu Jen Catholic University, Taipei 24205, Taiwan

¹¹Key Laboratory of Nuclear Physics and Ion-beam Application (MOE) and Institute of Modern Physics, Fudan University, Shanghai 200443, PR China

¹²Gifu University, Gifu 501-1193, Japan

¹³SOKENDAI (The Graduate University for Advanced Studies), Hayama 240-0193, Japan

¹⁴Gyeongsang National University, Jinju 52828, South Korea

¹⁵Department of Physics and Institute of Natural Sciences, Hanyang University, Seoul 04763, South Korea

¹⁶University of Hawaii, Honolulu, HI 96822, USA

¹⁷High Energy Accelerator Research Organization (KEK), Tsukuba 305-0801, Japan

¹⁸J-PARC Branch, KEK Theory Center, High Energy Accelerator Research Organization (KEK), Tsukuba 305-0801, Japan

¹⁹Higher School of Economics (HSE), Moscow 101000, Russian Federation

²⁰Forschungszentrum Jülich, 52425 Jülich, Germany

²¹IKERBASQUE, Basque Foundation for Science, 48013 Bilbao, Spain

²²Indian Institute of Science Education and Research Mohali, SAS Nagar, 140306, India

²³Indian Institute of Technology Guwahati, Assam 781039, India

²⁴Indian Institute of Technology Hyderabad, Telangana 502285, India

²⁵Indian Institute of Technology Madras, Chennai 600036, India

²⁶Indiana University, Bloomington, IN 47408, USA

- ²⁷*Institute of High Energy Physics, Chinese Academy of Sciences, Beijing 100049, PR China*
- ²⁸*Institute for High Energy Physics, Protvino 142281, Russian Federation*
- ²⁹*Institute of High Energy Physics, Vienna 1050, Austria*
- ³⁰*INFN - Sezione di Napoli, 80126 Napoli, Italy*
- ³¹*INFN - Sezione di Torino, 10125 Torino, Italy*
- ³²*Advanced Science Research Center, Japan Atomic Energy Agency, Naka 319-1195, Japan*
- ³³*J. Stefan Institute, 1000 Ljubljana, Slovenia*
- ³⁴*Institut für Experimentelle Teilchenphysik, Karlsruher Institut für Technologie, 76131 Karlsruhe, Germany*
- ³⁵*Kavli Institute for the Physics and Mathematics of the Universe (WPI), University of Tokyo, Kashiwa 277-8583, Japan*
- ³⁶*Department of Physics, Faculty of Science, King Abdulaziz University, Jeddah 21589, Saudi Arabia*
- ³⁷*Kitasato University, Sagami-hara 252-0373, Japan*
- ³⁸*Korea Institute of Science and Technology Information, Daejeon 34141, South Korea*
- ³⁹*Korea University, Seoul 02841, South Korea*
- ⁴⁰*Kyoto Sangyo University, Kyoto 603-8555, Japan*
- ⁴¹*Kyungpook National University, Daegu 41566, South Korea*
- ⁴²*Université Paris-Saclay, CNRS/IN2P3, IJCLab, 91405 Orsay, France*
- ⁴³*P.N. Lebedev Physical Institute of the Russian Academy of Sciences, Moscow 119991, Russian Federation*
- ⁴⁴*Liaoning Normal University, Dalian 116029, China*
- ⁴⁵*Faculty of Mathematics and Physics, University of Ljubljana, 1000 Ljubljana, Slovenia*
- ⁴⁶*Ludwig Maximilians University, 80539 Munich, Germany*
- ⁴⁷*Luther College, Decorah, IA 52101, USA*
- ⁴⁸*Malaviya National Institute of Technology Jaipur, Jaipur 302017, India*
- ⁴⁹*University of Maribor, 2000 Maribor, Slovenia*
- ⁵⁰*Max-Planck-Institut für Physik, 80805 München, Germany*
- ⁵¹*School of Physics, University of Melbourne, Victoria 3010, Australia*
- ⁵²*University of Mississippi, University, MS 38677, USA*
- ⁵³*University of Miyazaki, Miyazaki 889-2192, Japan*
- ⁵⁴*Moscow Physical Engineering Institute, Moscow 115409, Russian Federation*
- ⁵⁵*Graduate School of Science, Nagoya University, Nagoya 464-8602, Japan*
- ⁵⁶*Kobayashi-Maskawa Institute, Nagoya University, Nagoya 464-8602, Japan*
- ⁵⁷*Università di Napoli Federico II, 80126 Napoli, Italy*
- ⁵⁸*Nara Women's University, Nara 630-8506, Japan*
- ⁵⁹*National Central University, Chung-li 32054, Taiwan*
- ⁶⁰*National United University, Miao Li 36003, Taiwan*
- ⁶¹*Department of Physics, National Taiwan University, Taipei 10617, Taiwan*
- ⁶²*H. Niewodniczanski Institute of Nuclear Physics, Krakow 31-342, Poland*
- ⁶³*Nippon Dental University, Niigata 951-8580, Japan*
- ⁶⁴*Niigata University, Niigata 950-2181, Japan*
- ⁶⁵*University of Nova Gorica, 5000 Nova Gorica, Slovenia*
- ⁶⁶*Novosibirsk State University, Novosibirsk 630090, Russian Federation*

- ⁶⁷ *Osaka City University, Osaka 558-8585, Japan*
- ⁶⁸ *Pacific Northwest National Laboratory, Richland, WA 99352, USA*
- ⁶⁹ *Panjab University, Chandigarh 160014, India*
- ⁷⁰ *Peking University, Beijing 100871, PR China*
- ⁷¹ *University of Pittsburgh, Pittsburgh, PA 15260, USA*
- ⁷² *Research Center for Nuclear Physics, Osaka University, Osaka 567-0047, Japan*
- ⁷³ *Meson Science Laboratory, Cluster for Pioneering Research, RIKEN, Saitama 351-0198, Japan*
- ⁷⁴ *Department of Modern Physics and State Key Laboratory of Particle Detection and Electronics, University of Science and Technology of China, Hefei 230026, PR China*
- ⁷⁵ *Seoul National University, Seoul 08826, South Korea*
- ⁷⁶ *Showa Pharmaceutical University, Tokyo 194-8543, Japan*
- ⁷⁷ *Soochow University, Suzhou 215006, China*
- ⁷⁸ *Soongsil University, Seoul 06978, South Korea*
- ⁷⁹ *Sungkyunkwan University, Suwon 16419, South Korea*
- ⁸⁰ *School of Physics, University of Sydney, New South Wales 2006, Australia*
- ⁸¹ *Department of Physics, Faculty of Science, University of Tabuk, Tabuk 71451, Saudi Arabia*
- ⁸² *Tata Institute of Fundamental Research, Mumbai 400005, India*
- ⁸³ *Department of Physics, Technische Universität München, 85748 Garching, Germany*
- ⁸⁴ *School of Physics and Astronomy, Tel Aviv University, Tel Aviv 69978, Israel*
- ⁸⁵ *Toho University, Funabashi 274-8510, Japan*
- ⁸⁶ *Department of Physics, Tohoku University, Sendai 980-8578, Japan*
- ⁸⁷ *Earthquake Research Institute, University of Tokyo, Tokyo 113-0032, Japan*
- ⁸⁸ *Department of Physics, University of Tokyo, Tokyo 113-0033, Japan*
- ⁸⁹ *Tokyo Institute of Technology, Tokyo 152-8550, Japan*
- ⁹⁰ *Tokyo Metropolitan University, Tokyo 192-0397, Japan*
- ⁹¹ *Utkal University, Bhubaneswar 751004, India*
- ⁹² *Virginia Polytechnic Institute and State University, Blacksburg, VA 24061, USA*
- ⁹³ *Wayne State University, Detroit, MI 48202, USA*
- ⁹⁴ *Yamagata University, Yamagata 990-8560, Japan*
- ⁹⁵ *Yonsei University, Seoul 03722, South Korea*

ABSTRACT: We present a search for the dark photon A' in the $B^0 \rightarrow A'A'$ decays, where A' subsequently decays to e^+e^- , $\mu^+\mu^-$, and $\pi^+\pi^-$. The search is performed by analyzing 772×10^6 $B\bar{B}$ events collected by the Belle detector at the KEKB e^+e^- energy-asymmetric collider at the $\Upsilon(4S)$ resonance. No signal is found in the dark photon mass range $0.01 \text{ GeV}/c^2 \leq m_{A'} \leq 2.62 \text{ GeV}/c^2$, and we set upper limits of the branching fraction of $B^0 \rightarrow A'A'$ at the 90% confidence level. The products of branching fractions, $\mathcal{B}(B^0 \rightarrow A'A') \times \mathcal{B}(A' \rightarrow e^+e^-)^2$ and $\mathcal{B}(B^0 \rightarrow A'A') \times \mathcal{B}(A' \rightarrow \mu^+\mu^-)^2$, have limits of the order of 10^{-8} depending on the A' mass. Furthermore, considering A' decay rate to each pair of charged particles, the upper limits of $\mathcal{B}(B^0 \rightarrow A'A')$ are of the order of 10^{-8} – 10^{-5} . From the upper limits of $\mathcal{B}(B^0 \rightarrow A'A')$, we obtain the Higgs portal coupling for each assumed dark photon and dark Higgs mass. The Higgs portal couplings are of the order of 10^{-2} – 10^{-1} at $m_{h'} \simeq m_{B^0} \pm 40 \text{ MeV}/c^2$ and 10^{-1} – 1 at $m_{h'} \simeq m_{B^0} \pm 3 \text{ GeV}/c^2$.

KEYWORDS: e^+e^- Experiments, B physics, Beyond Standard Model, Branching fraction

Contents

1	Introduction	1
1.1	Branching fraction of dark photon decay	2
1.2	The SM expectation of B^0 decays to four charged leptons	2
2	The Belle detector	3
3	Signal event selection	3
4	Systematic uncertainties	5
5	Results	7
6	Conclusions	11

1 Introduction

The validity of the Standard Model (SM) has been confirmed by various experimental measurements [1], but it is also known that the SM is incomplete and cannot explain several phenomena occurring in nature, e.g. neutrino oscillations [2, 3] and the baryon asymmetry [4]. A possible way to explain the above problems while keeping the internal structure of the SM unaffected is to introduce a dark sector [5] that interacts with the SM particles only very weakly. For example, a vector mediator of hypothetical $U'(1)$ gauge interaction in the dark sector, the so-called dark photon, may interact with matter through various portals with a small coupling strength [6–8]. Such a model of the dark sector with portal interaction to the SM could explain the muon $g-2$ anomaly [9–12], baryogenesis [13], and high energy positron fraction anomaly in cosmic rays [14–18].

In this paper, we report a search for the dark photon A' , in the decays of B^0 mesons by analyzing the e^+e^- collision data from the Belle experiment. In particular, we study B^0 decays into a pair of dark photons, $B^0 \rightarrow A'A'$, which are mediated by an off-shell dark Higgs h' [5] (Fig. 1), wherein we scan the A' mass range between $0.01 \text{ GeV}/c^2$ and $2.62 \text{ GeV}/c^2$ in $10 \text{ MeV}/c^2$ ($m_{A'} < 1.1 \text{ GeV}/c^2$) and $20 \text{ MeV}/c^2$ ($m_{A'} > 1.1 \text{ GeV}/c^2$) intervals. Throughout the paper, the charge-conjugate modes are always implied. In this paper, we restrict ourselves to the hypothesis that all dark-sector particles coupling to A' are heavier than A' , therefore the latter can only decay to SM particles. Moreover, we assume that the A' decays promptly. In the kinematic range of this analysis, the allowed A' decay are to e^+e^- , $\mu^+\mu^-$, or hadronic final states. Lepton-flavor-violating decays [19, 20] $A' \rightarrow e^\pm\mu^\mp$ are not considered in this analysis.

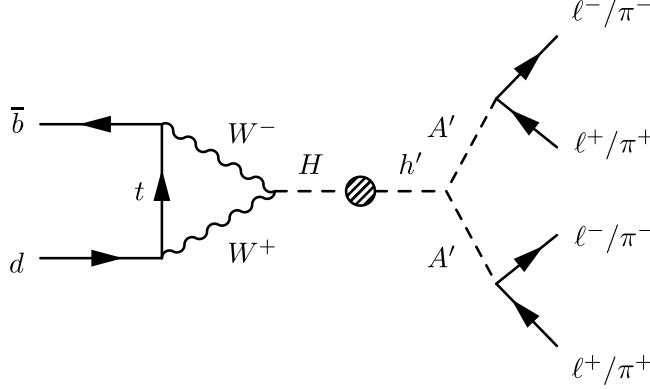


Figure 1. A possible diagram of $B^0 \rightarrow A'A'$ decay through off-shell Higgs–dark Higgs mixing indicated by the shaded circle.

1.1 Branching fraction of dark photon decay

In order to obtain $\mathcal{B}(B^0 \rightarrow A'A')$ from the analysis of the decays into the final states considered, we need to know the branching fractions of A' to a particular final state. Below the $\tau^+\tau^-$ threshold, the branching fraction of the dark photon that is consistent with our hypothesis is obtained as

$$\mathcal{B}(A' \rightarrow \ell^+\ell^-/\pi^+\pi^-) = \frac{\Gamma_{A' \rightarrow \ell^+\ell^-/\pi^+\pi^-}}{\Gamma_{A' \rightarrow e^+e^-} + \Gamma_{A' \rightarrow \mu^+\mu^-} + \Gamma_{A' \rightarrow \text{hadrons}}}, \quad (1.1)$$

where $\ell = e$ or μ . Following Ref. [21], we write down the partial widths to $\ell^+\ell^-$ and hadrons as

$$\begin{aligned} \Gamma_{A' \rightarrow \ell^+\ell^-} &= \frac{1}{3} \alpha \varepsilon_{\text{mix}}^2 m_{A'} \sqrt{1 - 4m_\ell^2/m_{A'}^2} (1 + 2m_\ell^2/m_{A'}^2), \\ \Gamma_{A' \rightarrow \text{hadrons}} &= \Gamma_{A' \rightarrow \mu^+\mu^-} \times R(s = m_{A'}^2), \end{aligned} \quad (1.2)$$

with the square of the total center-of-mass (CM) frame energy s , the kinetic mixing parameter ε_{mix} , and $R(s) = \sum_{e^+e^- \rightarrow \text{hadrons}} / \sum_{e^+e^- \rightarrow \mu^+\mu^-}$ which is determined by various experiments [1]. The branching fraction of $A' \rightarrow \pi^+\pi^-$ is then obtained as [22]:

$$\mathcal{B}(A' \rightarrow \pi^+\pi^-) = \mathcal{B}(A' \rightarrow \text{hadrons}) \times \sum (e^+e^- \rightarrow \pi^+\pi^-) / \sum (e^+e^- \rightarrow \text{hadrons}). \quad (1.3)$$

1.2 The SM expectation of B^0 decays to four charged leptons

The B^0 -decay final states that we analyze are $e^+e^-e^+e^-$, $e^+e^-\mu^+\mu^-$, $\mu^+\mu^-\mu^+\mu^-$, $e^+e^-\pi^+\pi^-$, and $\mu^+\mu^-\pi^+\pi^-$. In the SM, branching fractions of B^0 -meson decays to four-charged-lepton final states are expected to be $\mathcal{O}(10^{-12})$ [23]. Due to the low SM signal and background yields expected, these multileptonic B -meson decay channels can be a sensitive probe for dark sector bosons. The LHCb experiment has set an upper limit $\mathcal{B}(B^0 \rightarrow \mu^+\mu^-\mu^+\mu^-) < 6.9 \times 10^{-10}$ at 95% confidence level (C.L.) [24] and measured $\mathcal{B}(B^0 \rightarrow \mu^+\mu^-\pi^+\pi^-) = (2.1 \pm 0.5) \times 10^{-8}$ [25].

2 The Belle detector

Our analysis is based on the full 711 fb^{-1} integrated luminosity of the $\Upsilon(4S)$ data set from the Belle detector [26, 27] at KEKB e^+e^- energy-asymmetric collider [28, 29]. The Belle detector consists of seven subdetectors with 1.5 T magnetic field along the beam axis. Inside the coil, there are the silicon vertex detector, the central drift chamber (CDC), the aerogel threshold Cherenkov counters (ACC), the time-of-flight scintillation counters (TOF), and the electromagnetic calorimeter (ECL). In the return yoke outside the coil, a K_L^0 meson and muon detector (KLM) is instrumented.

We perform a blind search in this analysis, for which we generate Monte Carlo (MC) simulation samples using EvtGen [30] for event generation and GEANT3 [31] for detector simulation. Signal efficiencies are determined from the signal MC set, where one million events are generated for each signal mode and dark photon mass. The event shape and amount of the background events are studied by using generic MC samples simulating $e^+e^- \rightarrow \Upsilon(4S) \rightarrow B\bar{B}$ and $e^+e^- \rightarrow q\bar{q}$ ($q = u, d, s, c$) (‘continuum’) processes. The size of MC samples for $\Upsilon(4S)$ and continuum simulation corresponds to 10 and 6 times that of real data, respectively.

3 Signal event selection

To select signal events, we retain tracks satisfying the following track reconstruction quality requirements. Because we assume prompt dark photon decays, all tracks are required to originate from near the interaction point (IP). In particular, each track should satisfy the following conditions on the impact parameters in the transverse and longitudinal directions, $dr < 0.2 \text{ cm}$ and $|dz| < 3.0 \text{ cm}$, respectively. The impact parameters are calculated using the beam IP and track helix, and the z -axis is aligned opposite the direction of positron beam. We also require a good track fit based upon χ^2 per degree of freedom ($N_{\text{d.o.f.}}$) by accepting only the tracks with $\chi^2/N_{\text{d.o.f.}} < 5$.

The species of the charged particles are identified by considering the likelihood ratios. Muons are identified by requiring $\mathcal{L}_\mu/(\mathcal{L}_\mu + \mathcal{L}_K + \mathcal{L}_\pi) > 0.9$, where the likelihood \mathcal{L}_j ($j = \mu, K, \pi$) [32] is constructed by the hit position and penetration in the KLM. Electrons are required to meet $\mathcal{L}_e/(\mathcal{L}_e + \mathcal{L}_{\text{not-}e}) > 0.9$ where the likelihood \mathcal{L}_j ($j = e, \text{not-}e$) [33] is determined by dE/dx from the CDC, ratio of the ECL cluster energy to the matched track momentum, shower shape of the ECL cluster, and the ACC photoelectron response. Charged pions and kaons are identified by the likelihood [34] using the dE/dx from the CDC, the ACC photoelectron response, and the time-of-flight information from the TOF. The tracks with $\mathcal{L}_\pi/(\mathcal{L}_K + \mathcal{L}_\pi) > 0.4$ are identified as pions.

To recover energy losses by e^\pm candidates due to bremsstrahlung, radiative photons are added to the electron momentum if they fall within a 0.05 radian cone around the e^\pm direction. We require these photons to exceed an energy threshold that depends on the ECL region: $E_\gamma > 50$ (barrel), 100 (forward endcap), and 150 (backward endcap) MeV.

The dark photon candidate is reconstructed in the following modes: $A' \rightarrow e^+e^-$, $\mu^+\mu^-$, and $\pi^+\pi^-$. For $B^0 \rightarrow e^+e^-e^+e^-$ and $\mu^+\mu^-\mu^+\mu^-$ modes, we have an ambiguity between

$(\ell_1^+ \ell_1^-)(\ell_2^+ \ell_2^-)$ and $(\ell_1^+ \ell_2^-)(\ell_2^+ \ell_1^-)$, where the lepton pair from a single A' decay is indicated in parentheses. To find a single dark photon combination per event, we choose that corresponding to the smallest invariant mass difference of dark photon candidates, $\Delta M_{A'}$.

Finally, B^0 candidates are reconstructed from two dark photon candidates. To extract signal events from data, we use the following five variables, defined in the CM frame: M_{bc} , ΔE , E_{miss} , $\Delta M_{A'}$, and $\sum \delta M_{A'}$. $M_{bc} \equiv \sqrt{(\sqrt{s}/2)^2 - \vec{p}_B^2}$ is the beam-energy-constrained mass, where \vec{p}_B is the momentum of the reconstructed B^0 . $\Delta E \equiv E_{B^0} - (\sqrt{s}/2)$ is the difference between the B^0 -candidate energy and the beam energy ($= \sqrt{s}/2$), and E_{miss} is the missing energy, $E_{\text{miss}} \equiv \sqrt{s} - \sum_j E_j$ where the index j is for all charged and neutral particles in the event. The missing energy is useful to reduce combinatorial background due to multiple semileptonic decays from $b \rightarrow c\ell^-\bar{\nu}_\ell$ and $c \rightarrow (s, d)\ell^+\nu_\ell$ for both B and \bar{B} . For the two dark photon candidates in an event, we calculate $\Delta M_{A'} \equiv |M_{A'_1} - M_{A'_2}|$ and $\sum \delta M_{A'} \equiv |(M_{A'_1} - m_{A'}^{\text{bin}}) + (M_{A'_2} - m_{A'}^{\text{bin}})|$, where $M_{A'_j}$ is the reconstructed mass of A'_j ($j = 1, 2$) and $m_{A'}^{\text{bin}}$ is the nominal A' mass for a particular bin of $m_{A'}$.

For the signal event selection, we require $M_{bc} > 5.27 \text{ GeV}/c^2$ and $E_{\text{miss}} < 3.5 \text{ GeV}$ for all modes. Considering the energy loss from e^\pm , ΔE requirements are chosen separately for different modes: $-0.2 \text{ GeV} < \Delta E < 0.05 \text{ GeV}$ for $B^0 \rightarrow e^+e^-e^+e^-$, $-0.1 \text{ GeV} < \Delta E < 0.04 \text{ GeV}$ for $B^0 \rightarrow e^+e^-\mu^+\mu^-$ and $e^+e^-\pi^+\pi^-$, and $-0.03 \text{ GeV} < \Delta E < 0.03 \text{ GeV}$ for $B^0 \rightarrow \mu^+\mu^-\mu^+\mu^-$ and $\mu^+\mu^-\pi^+\pi^-$. We use $\Delta M_{A'}$ and $\sum \delta M_{A'}$ to set the search window for each $m_{A'}^{\text{bin}}$ and the final-state mode. The requirements on these variables depend on both $m_{A'}^{\text{bin}}$ and the number of electrons in the final state. For $m_{A'}^{\text{bin}} > 0.1 \text{ GeV}/c^2$, we require $\Delta M_{A'}(\sum \delta M_{A'}) < 0.06 \times m_{A'}^{\text{bin}} + 0.03 \text{ GeV}/c^2$ for $B^0 \rightarrow e^+e^-e^+e^-$, $\Delta M_{A'}(\sum \delta M_{A'}) < 0.03 \times m_{A'}^{\text{bin}} + 0.01 \text{ GeV}/c^2$ for $B^0 \rightarrow e^+e^-\mu^+\mu^-$ and $e^+e^-\pi^+\pi^-$, and $\Delta M_{A'}(\sum \delta M_{A'}) < 0.01 \times m_{A'}^{\text{bin}} + 0.01 \text{ GeV}/c^2$ for $B^0 \rightarrow \mu^+\mu^-\mu^+\mu^-$ and $\mu^+\mu^-\pi^+\pi^-$. The above conditions are determined so that if we consider the distribution of $\Delta M_{A'}$ the upper edge of the accepted region has a value of nearly 3–5% of the peak value. In addition, we make use of the approximately linear increase of the $\Delta M_{A'}$ width as a function of $m_{A'}^{\text{bin}}$. We choose the same selection for $\sum \delta M_{A'}$ since the distribution is almost the same as $\Delta M_{A'}$. For $m_{A'}^{\text{bin}} \leq 0.1 \text{ GeV}/c^2$, we apply slightly different selection conditions for $\Delta M_{A'}$ and $\sum \delta M_{A'}$, while requirements on M_{bc} and ΔE remain the same as for $m_{A'}^{\text{bin}} > 0.1 \text{ GeV}/c^2$. We do not use E_{miss} for $m_{A'}^{\text{bin}} \leq 0.1 \text{ GeV}/c^2$, because for such low-mass dark photons, little background is expected from generic B decays. For $m_{A'}^{\text{bin}} \leq 0.1 \text{ GeV}/c^2$, the resolutions of both $\Delta M_{A'}$ and $\sum \delta M_{A'}$ are nearly independent of $m_{A'}^{\text{bin}}$. Therefore, we require $\Delta M_{A'} < 0.02 \text{ GeV}/c^2$ and $\sum \delta M_{A'} < 0.02 \text{ GeV}/c^2$ for all $m_{A'} \leq 0.1 \text{ GeV}/c^2$. From the MC study, our $\Delta M_{A'}$ selections in $A' \rightarrow \mu^+\mu^-$ and $\pi^+\pi^-$ cover roughly ± 2.5 times the mass resolution. In case of $A' \rightarrow e^+e^-$, the mass resolution is worse, and our selections correspond to $\pm(1.7 - 2.5)$ times the mass resolution, depending on $m_{A'}$. For instance, the $M_{A'}$ resolution of the 1.5 GeV dark photon is about 5 MeV for $A' \rightarrow \mu^+\mu^-$ or $\pi^+\pi^-$, while for $A' \rightarrow e^+e^-$ it is about 20 MeV. The union of the search windows determined using $\Delta M_{A'}$ and $\sum \delta M_{A'}$ for all $m_{A'}^{\text{bin}}$ covers the entire dark photon mass range of our study without any gap.

The dominant SM background sources for $\ell^+\ell^-$ pairs are photon conversion and charmonium meson decays, mostly J/ψ and $\psi(2S)$. To reduce the background events from

photon conversion, e^+e^- pairs with $M_{e^+e^-} < 0.1 \text{ GeV}/c^2$ are rejected when we search for $m_{A'} > 0.1 \text{ GeV}/c^2$. On the other hand, this veto is not applied for the searches in the region $m_{A'} \leq 0.1 \text{ GeV}/c^2$. To suppress the lepton pairs from charmonium decays such as J/ψ or $\psi(2S) \rightarrow \ell^+\ell^-$, we reject two regions: $3.00(3.05) \text{ GeV}/c^2 < M_{e^+e^-(\mu^+\mu^-)} < 3.15(3.13) \text{ GeV}/c^2$ for J/ψ and $3.60(3.65) \text{ GeV}/c^2 < M_{e^+e^-(\mu^+\mu^-)} < 3.75(3.73) \text{ GeV}/c^2$ for $\psi(2S)$.

For the charged pion pairs, there is strong background from light mesons, such as K_S^0 , ρ^0 , and $f_0(980)$. Because of possible $K-\pi$ misidentification, K^{*0} , ϕ and so on are also a source of possible background. Since production of such mesons is copious, especially that of ρ^0 mesons, we reject the $0.45 \text{ GeV}/c^2 < M_{\pi^+\pi^-} < 1.1 \text{ GeV}/c^2$. Another source of pion pairs is D^0 meson. Two decay channels, $D^0 \rightarrow \pi^+\pi^-$ and $D^0 \rightarrow \pi^+K^-$ are considered. A direct D^0 veto is applied by removing $\pi^+\pi^-$ combinations which satisfy $1.85 \text{ GeV}/c^2 < M_{\pi^+\pi^-} < 1.88 \text{ GeV}/c^2$. The other decay channel, $D^0 \rightarrow \pi^+K^-$, can mimic the signal via $K-\pi$ misidentification. We reject these events by discarding the $1.85 \text{ GeV}/c^2 < M_{\pi^+K^-} < 1.88 \text{ GeV}/c^2$ mass range.

After signal selection, most of the combinatorial background is in the $B^0 \rightarrow \ell^+\ell^-\pi^+\pi^-$ mode, coming from the continuum processes $e^+e^- \rightarrow q\bar{q}$ ($q = u, d, s$ or c). In the four-lepton mode, on the other hand, there is almost no background left. The continuum background is suppressed via multivariate analysis (MVA) using the Fisher discriminant [35] method in the TMVA [36] package. We make use of 16 event shape variables: the cosine of angle between the beam axis and B^0 momentum ($\cos\theta_B$), the cosine of angle between the thrust axis of the B^0 daughters and that of the rest of the event ($\cos\theta_T$), and the Fisher discriminant components of modified Fox-Wolfram moments [37]. The MVA training is performed for the $\ell^+\ell^-\pi^+\pi^-$ final state for each $m_{A'}^{\text{bin}}$, using the signal and continuum MC. We apply MVA selection criteria to retain from 75% to 90% of signal and from 10% to 30% of continuum background, depending on $m_{A'}$ and final state.

4 Systematic uncertainties

We determine the branching fraction of $B^0 \rightarrow A'A'$ as

$$\mathcal{B}(B^0 \rightarrow A'A') = \frac{N_{\text{obs}} - N_{\text{bkg}}}{\epsilon \times 2 \times N_{B\bar{B}} \times \mathcal{B}_0}, \quad (4.1)$$

where \mathcal{B}_0 is the branching fraction of $\Upsilon(4S) \rightarrow B^0\bar{B}^0$, of which the current world-average value is 0.486 ± 0.006 [1], N_{obs} is the yield, N_{bkg} is the number of expected background events determined from MC, ϵ is the signal reconstruction efficiency considering branching fraction of A' subdecays, and $N_{B\bar{B}} = (772 \pm 11) \times 10^6$ is the number of $B\bar{B}$ pairs which are collected by the Belle detector.

The most important source of systematic uncertainties is the signal reconstruction efficiency, which is obtained by MC. The sources of uncertainty include the statistical error in the signal MC, track reconstruction efficiency, particle identification (PID) efficiency, and uncertainties in the MVA method used to suppress continuum background for $\ell^+\ell^-\pi^+\pi^-$

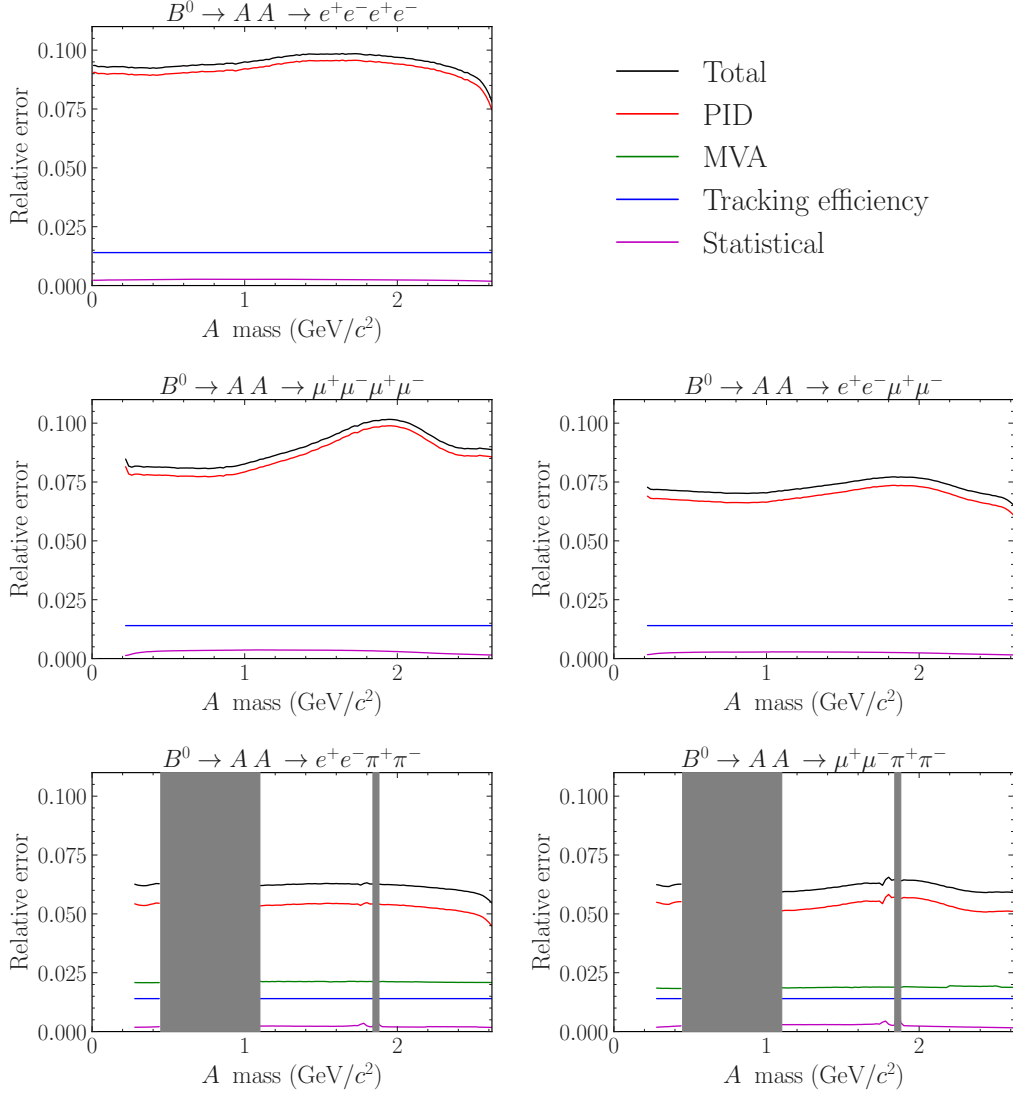


Figure 2. Relative uncertainty of signal reconstruction efficiency for each A' mass and final state.

final states. The uncertainties for $N_{B\bar{B}}$ and \mathcal{B}_0 also contribute to systematics. The uncertainties due to background estimation are very small compared to other systematic uncertainties.

Track reconstruction efficiency is studied using the decay chain $D^{*+} \rightarrow D^0\pi^+$, $D^0 \rightarrow K_S^0\pi^+\pi^-$, and $K_S^0 \rightarrow \pi^+\pi^-$ where we tag all the charged tracks in the chain but one from K_S^0 decays ('test track') then try to find the test track. We compare the tracking efficiency difference of the test track for both data and MC. The error is 1.4%, independent of the dark photon mass and final state.

The PID correction is applied to each daughter electron, muon, and pion. The lepton

(pion) identification correction is studied using the difference between MC and data for the process $\gamma\gamma \rightarrow e^+e^-/\mu^+\mu^-$ ($D^{*+} \rightarrow D^0\pi_{\text{slow}}^+ \rightarrow K^-\pi^+\pi_{\text{slow}}^+$), and the errors are approximately 2% (1%) per lepton (pion), with the resulting correction factor being about 90%. The exact correction factor and uncertainty depend on $m_{A'}$ through different kinematics.

The MVA correction factor and uncertainty are studied using the control mode, $B^0 \rightarrow J/\psi K^{*0} \rightarrow e(\mu)^+e(\mu)^-\pi^-K^+$. We apply MVA training results for the continuum suppression of $\ell^+\ell^-\pi^+\pi^-$ modes for each assumed value of $m_{A'}$ to $B^0 \rightarrow J/\psi K^{*0}$ MC and data. We then calculate the double ratio $(N_{\text{data,A}}/N_{\text{data,B}})/(N_{\text{MC,A}}/N_{\text{MC,B}})$, where $N_{\text{data(MC),B}}$ and $N_{\text{data(MC),A}}$ are the number of signal candidates in data(MC) before and after MVA training application, respectively. The systematic uncertainty due to MVA training is taken from the uncertainties in the double ratio, and these uncertainties are approximately 2% at all values of $m_{A'}$.

After multiplying all correction factors, signal efficiencies are mostly 5 – 20%. The efficiencies increase as the A' mass approaches 0 or $m_{B^0}/2$, in which case both e^\pm (μ^\pm) from the A' decays are more likely to exceed the energy threshold for ECL (KLM) detection. The summary of signal-efficiency-related systematic uncertainties is shown in Fig. 2, and the total systematic uncertainties are 7.5–10% for $e^+e^-e^+e^-$ and $\mu^+\mu^-\mu^+\mu^-$ final states and 5–7.5% for $e^+e^-\mu^+\mu^-$, $e^+e^-\pi^+\pi^-$, and $\mu^+\mu^-\pi^+\pi^-$ final states.

5 Results

Figure 3 shows the number of $B^0 \rightarrow A'A'$ candidate events. There are no events observed in any bin in the $e^+e^-\mu^+\mu^-$ and $\mu^+\mu^-\mu^+\mu^-$ mode, while we find $N_{\text{obs}} \leq 2$ events for $e^+e^-e^+e^-$, $e^+e^-\pi^+\pi^-$, and $\mu^+\mu^-\pi^+\pi^-$ modes. The yields are consistent with the expected number of background events and we set the upper limits at 90% C.L.

For the limits of $\mathcal{B}(B^0 \rightarrow A'A')$, we combine the number of expected background events, signal candidates in data, and signal reconstruction efficiencies of the five final states. The combined numbers of expected background events and signal candidates in data are calculated by simply adding the results for the individual final states. For the signal efficiencies, we first obtain the ratio $F_f \equiv \mathcal{B}(B^0 \rightarrow A'A' \rightarrow f)/\mathcal{B}(B^0 \rightarrow A'A')$, where f is each final state, using Eq. (1.1). In case of $e^+e^-\mu^+\mu^-$, for example, $F_{e^+e^-\mu^+\mu^-}$ is $2 \times \mathcal{B}(A' \rightarrow e^+e^-) \times \mathcal{B}(A' \rightarrow \mu^+\mu^-)$. The graph of F_f is presented in Fig. 4. With this ratio F_f , the combined efficiency is determined as $\sum_f \epsilon_f F_f$ where ϵ_f is the signal efficiency of the final state f . The upper limits are calculated using the POLE program [38], which is based on the Feldman-Cousins unified approach [39]. We report the limits on the products of branching fractions $\mathcal{B}(B^0 \rightarrow A'A') \times \mathcal{B}(A' \rightarrow e^+e^-)^2$ and $\mathcal{B}(B^0 \rightarrow A'A') \times \mathcal{B}(A' \rightarrow \mu^+\mu^-)^2$, as well as the limits on $\mathcal{B}(B^0 \rightarrow A'A')$. For $\mathcal{B}(B^0 \rightarrow A'A')$, we use Eq. (1.1) to combine the five final states. The upper limits of $\mathcal{B}(B^0 \rightarrow A'A')$ are obtained in the mass range $0.01 \text{ GeV}/c^2 \leq m_{A'} \leq 1.10 \text{ GeV}/c^2$ with $10 \text{ MeV}/c^2$ bin and $1.10 \text{ GeV}/c^2 \leq m_{A'} \leq 2.62 \text{ GeV}/c^2$ with $20 \text{ MeV}/c^2$ bin.

The obtained limits are shown in Fig. 5 as functions of $m_{A'}$. The limits on the products of branching fractions are $\mathcal{O}(10^{-8})$ for both modes and in all $m_{A'}$ bins. For $\mathcal{B}(B^0 \rightarrow A'A')$, the upper limits are $\mathcal{O}(10^{-8})$ – $\mathcal{O}(10^{-5})$. Due to the light meson veto in the $\ell^+\ell^-\pi^+\pi^-$ final

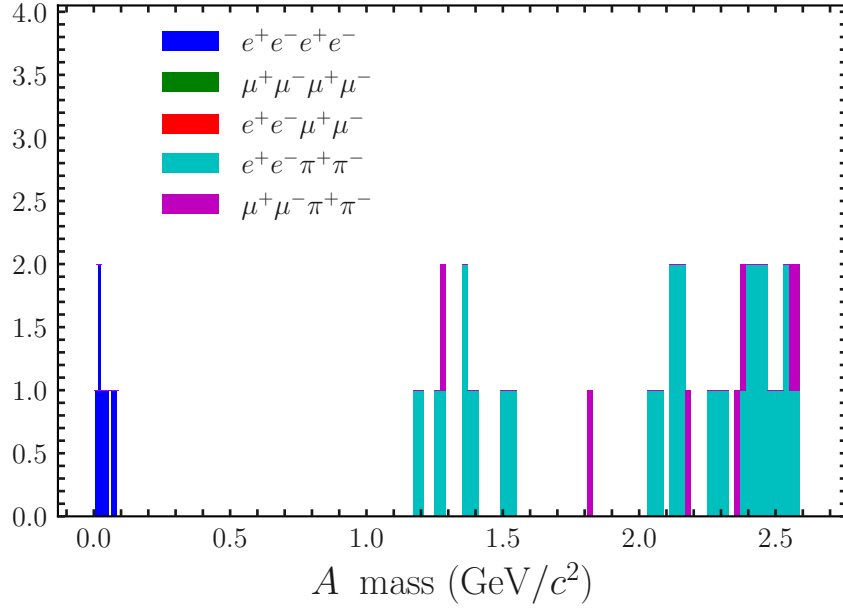


Figure 3. The number of $B^0 \rightarrow A'A'$ candidate events for each final state.

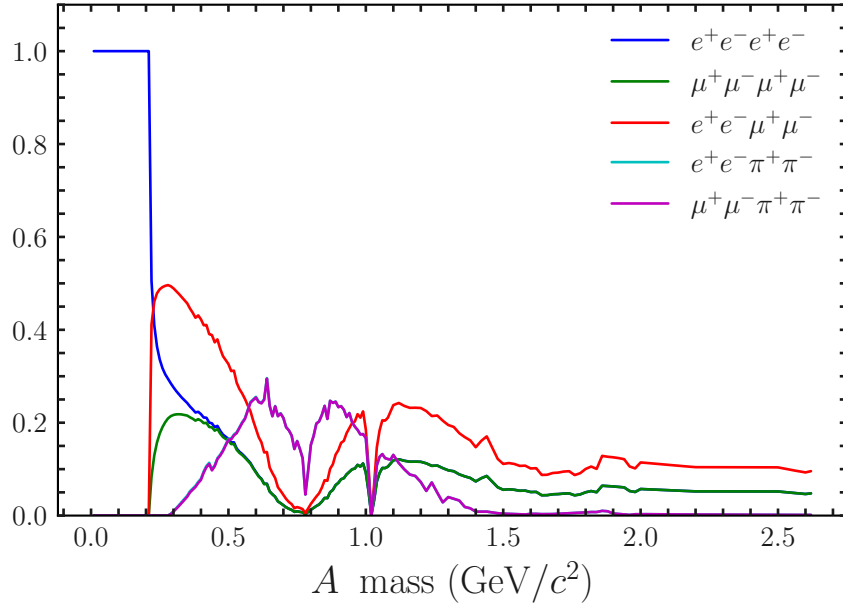


Figure 4. $\mathcal{B}(B^0 \rightarrow A'A' \rightarrow f)/\mathcal{B}(B^0 \rightarrow A'A')$ distributions for each final state and dark photon mass. $e^+e^-\pi^+\pi^-$ and $\mu^+\mu^-\pi^+\pi^-$ distributions are almost the same for the whole region. $e^+e^-e^+e^-$ and $\mu^+\mu^-\mu^+\mu^-$ distributions are the same and $e^+e^-\mu^+\mu^-$ distribution is twice that of four-electron or four-muon final states in the region $m_{A'} > 0.5 \text{ GeV}/c^2$.

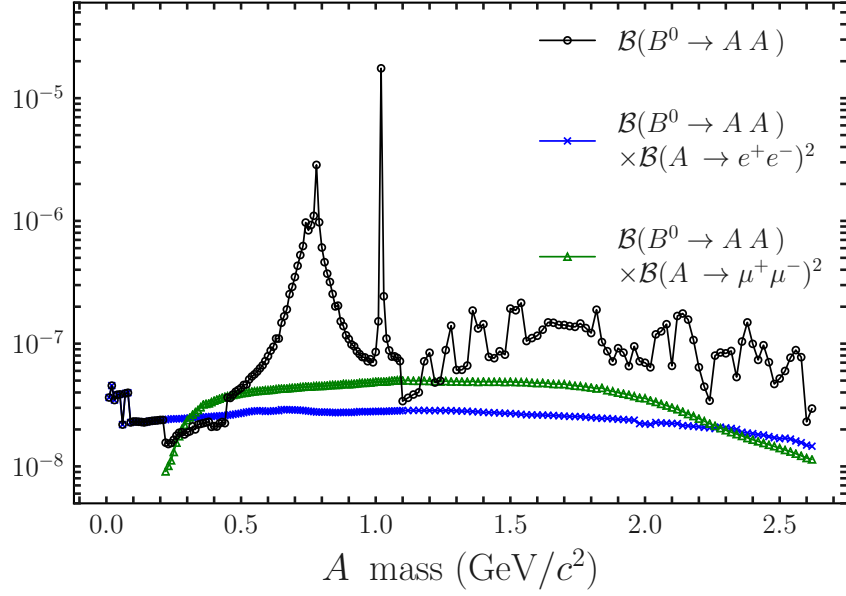


Figure 5. Upper limits of $B^0 \rightarrow A' A'$ branching fraction at 90% C.L.

states and the large fraction of $A' \rightarrow$ hadrons in the veto region from Eq. (1.1), the upper limits near the masses of ρ^0 and ϕ mesons are less restrictive than others. Table 1 lists the signal efficiency, the expected number of backgrounds and number of observed events (N_{obs}) for some of $m_{A'}$.

Table 1. Signal efficiency, expected the number of backgrounds, yields for each B^0 final state and upper limits of $B^0 \rightarrow A' A'$ branching fraction with 90% confidence interval. The table presents a part of the results for dark photons with (i) 20 MeV/ c^2 interval in $m_{A'} < 2m_\mu$ region, (ii) 100 MeV/ c^2 interval on the other region.

$m_{A'}$ (GeV/ c^2)	Eff. (%)	$e^+e^-e^+e^-$ $N_{\text{bkg}}^{\text{exp}}$	Yield	Yield Eff. (%)	$e^+e^- \mu^+\mu^-$ $N_{\text{bkg}}^{\text{exp}}$	Yield	Yield Eff. (%)	$\mu^+\mu^- \mu^+\mu^-$ $N_{\text{bkg}}^{\text{exp}}$	Yield	Yield Eff. (%)	$e^+e^- \pi^+\pi^-$ $N_{\text{bkg}}^{\text{exp}}$	Yield	Yield Eff. (%)	$\mu^+\mu^- \pi^+\pi^-$ $N_{\text{bkg}}^{\text{exp}}$	Yield	Yield Eff. (%)	90% U.L. (10^{-8})
0.02	14.82	0.83 ± 0.37	2	-	-	-	-	-	-	-	-	-	-	-	-	-	4.55
0.04	14.62	0.00 ± 0.17	1	-	-	-	-	-	-	-	-	-	-	-	-	-	3.85
0.06	14.40	0.00 ± 0.17	0	-	-	-	-	-	-	-	-	-	-	-	-	-	2.21
0.08	14.07	0.00 ± 0.17	1	-	-	-	-	-	-	-	-	-	-	-	-	-	4.00
0.10	13.63	0.00 ± 0.17	0	-	-	-	-	-	-	-	-	-	-	-	-	-	2.34
0.12	13.66	0.00 ± 0.17	0	-	-	-	-	-	-	-	-	-	-	-	-	-	2.33
0.14	13.85	0.00 ± 0.17	0	-	-	-	-	-	-	-	-	-	-	-	-	-	2.30
0.16	13.57	0.00 ± 0.17	0	-	-	-	-	-	-	-	-	-	-	-	-	-	2.35
0.18	13.37	0.00 ± 0.17	0	-	-	-	-	-	-	-	-	-	-	-	-	-	2.38
0.20	13.25	0.00 ± 0.17	0	-	-	-	-	-	-	-	-	-	-	-	-	-	2.41
0.30	12.78	0.00 ± 0.17	0	15.01	0.00 ± 0.17	0	15.01	0.00 ± 0.17	0	13.22	0.00 ± 0.17	0	21.16	0.00 ± 0.49	0	19.85	0.50 \pm 0.50
0.40	12.35	0.00 ± 0.17	0	12.44	0.00 ± 0.17	0	12.44	0.00 ± 0.17	0	9.18	0.00 ± 0.17	0	19.25	0.50 ± 0.50	0	15.30	0.00 ± 0.49
0.50	11.67	0.00 ± 0.17	0	11.39	0.00 ± 0.17	0	11.39	0.00 ± 0.17	0	7.98	0.00 ± 0.17	0	-	-	-	-	4.39
0.60	11.07	0.10 ± 0.19	0	10.71	0.00 ± 0.17	0	10.71	0.00 ± 0.17	0	7.53	0.00 ± 0.17	0	-	-	-	-	7.99
0.70	10.96	0.00 ± 0.17	0	10.46	0.00 ± 0.17	0	10.46	0.00 ± 0.17	0	7.18	0.00 ± 0.17	0	-	-	-	-	35.2
0.80	11.39	0.00 ± 0.17	0	10.54	0.00 ± 0.17	0	10.54	0.00 ± 0.17	0	6.97	0.00 ± 0.17	0	-	-	-	-	61.3
0.90	11.47	0.00 ± 0.17	0	10.45	0.00 ± 0.17	0	10.45	0.00 ± 0.17	0	6.73	0.00 ± 0.17	0	-	-	-	-	11.0
1.00	11.26	0.00 ± 0.17	0	10.20	0.00 ± 0.17	0	10.20	0.00 ± 0.17	0	6.42	0.00 ± 0.17	0	-	-	-	-	8.63
1.10	11.10	0.00 ± 0.17	0	9.91	0.00 ± 0.17	0	9.91	0.00 ± 0.17	0	6.27	0.00 ± 0.17	0	14.73	0.30 ± 0.52	0	9.87	0.50 ± 0.50
1.20	11.07	0.00 ± 0.17	0	9.88	0.00 ± 0.17	0	9.88	0.00 ± 0.17	0	6.34	0.00 ± 0.17	0	14.72	0.25 ± 0.51	1	9.87	0.00 ± 0.49
1.30	11.22	0.00 ± 0.17	0	10.10	0.00 ± 0.17	0	10.10	0.00 ± 0.17	0	6.40	0.00 ± 0.17	0	15.08	0.30 ± 0.52	0	9.81	0.00 ± 0.49
1.40	11.48	0.00 ± 0.17	0	10.18	0.10 ± 0.19	0	10.18	0.00 ± 0.17	0	6.44	0.00 ± 0.17	0	15.57	1.00 ± 0.55	1	9.76	0.00 ± 0.49
1.50	11.75	0.00 ± 0.17	0	10.37	0.00 ± 0.17	0	10.37	0.00 ± 0.17	0	6.45	0.00 ± 0.17	0	15.63	1.10 ± 0.56	1	9.94	0.00 ± 0.49
1.60	12.13	0.00 ± 0.17	0	10.57	0.00 ± 0.17	0	10.57	0.00 ± 0.17	0	6.62	0.00 ± 0.17	0	15.84	0.85 ± 0.53	0	9.44	0.00 ± 0.49
1.70	12.34	0.00 ± 0.17	0	10.86	0.00 ± 0.17	0	10.86	0.00 ± 0.17	0	6.78	0.00 ± 0.17	0	13.74	0.40 ± 0.53	0	8.68	0.00 ± 0.49
1.80	12.69	0.00 ± 0.17	0	11.42	0.00 ± 0.17	0	11.42	0.00 ± 0.17	0	7.24	0.00 ± 0.17	0	13.49	0.40 ± 0.53	0	8.58	0.00 ± 0.49
1.90	13.06	0.10 ± 0.19	0	12.02	0.00 ± 0.17	0	12.02	0.00 ± 0.17	0	7.94	0.00 ± 0.17	0	17.73	0.50 ± 0.54	0	12.91	0.00 ± 0.49
2.00	13.43	0.25 ± 0.22	0	13.08	0.00 ± 0.17	0	13.08	0.00 ± 0.17	0	8.84	0.00 ± 0.17	0	19.94	1.32 ± 0.57	0	14.62	0.10 ± 0.50
2.10	13.90	0.15 ± 0.20	0	14.39	0.00 ± 0.17	0	14.39	0.00 ± 0.17	0	10.52	0.00 ± 0.17	0	20.10	0.75 ± 0.56	0	16.28	0.27 ± 0.51
2.20	14.50	0.20 ± 0.22	0	16.20	0.10 ± 0.19	0	16.20	0.00 ± 0.17	0	12.87	0.00 ± 0.17	0	17.77	1.30 ± 0.61	0	17.76	0.00 ± 0.49
2.30	15.32	0.00 ± 0.17	0	18.47	0.10 ± 0.19	0	18.47	0.00 ± 0.17	0	16.01	0.00 ± 0.17	0	18.05	2.04 ± 0.63	1	19.74	0.20 ± 0.51
2.40	16.47	0.20 ± 0.22	0	20.79	0.00 ± 0.17	0	20.79	0.00 ± 0.17	0	19.21	0.00 ± 0.17	0	19.01	2.05 ± 0.66	2	20.87	0.72 ± 0.52
2.50	18.15	0.20 ± 0.22	0	23.24	0.00 ± 0.17	0	23.24	0.00 ± 0.17	0	22.40	0.00 ± 0.17	0	18.73	2.40 ± 0.66	1	23.08	0.50 ± 0.50
2.60	21.05	0.00 ± 0.17	0	26.34	0.10 ± 0.19	0	26.34	0.00 ± 0.17	0	26.85	0.00 ± 0.17	0	22.52	2.25 ± 0.79	0	25.34	1.52 ± 0.74

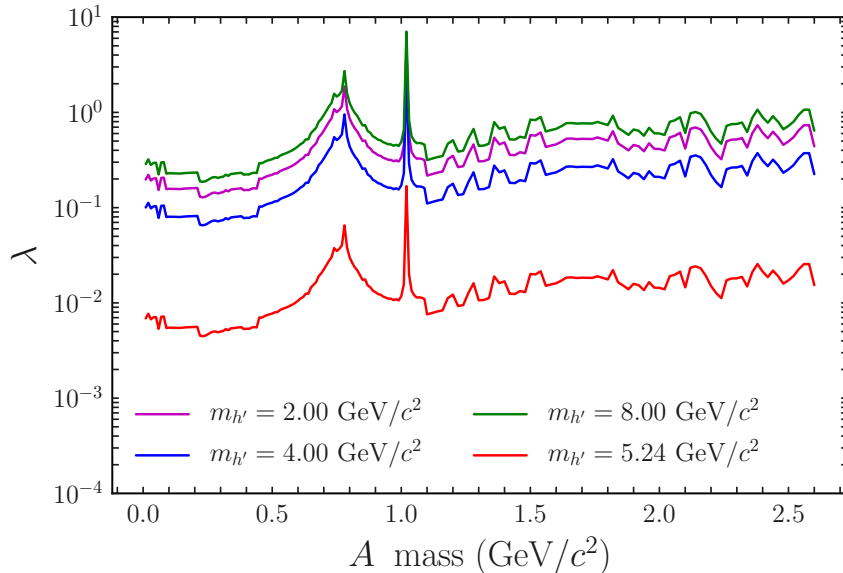


Figure 6. 90% upper limits of the Higgs portal coupling (λ) versus the dark photon mass for a 2.00, 4.00, 5.24, 8.00 GeV/c^2 dark Higgs.

The $B^0 \rightarrow A'A'$ branching fraction with off-shell H - h' mixing, for all but the $m_{h'} \sim m_{B^0}$ region, is calculated as [5]¹,

$$\mathcal{B}(B^0 \rightarrow A'A') \simeq 7 \times 10^{-7} \times \lambda^2 \times V_{A'A'}^{1/2} \times \frac{V_{A'A'} + 12m_{A'}^4/m_{B^0}^4}{(1 - m_{h'}^2/m_{B^0}^2)^2} \quad (5.1)$$

where λ is the Higgs portal coupling with a new scalar field H' from $\mathcal{L}_{\text{Higgs}} = -\lambda(H^\dagger H)(H'^\dagger H')$ and $V_{A'A'} = 1 - 4m_{A'}^2/m_{B^0}^2$. From Eq. (5.1) and the limits on $\mathcal{B}(B^0 \rightarrow A'A')$, we determine the 90% C.L. upper limits on λ versus $m_{A'}$ (Fig. 6) and $m_{h'}$ (Fig. 7). In the region where $m_{h'} \simeq m_{B^0}$, the upper limit on λ gets as low as $\mathcal{O}(10^{-2})$. Otherwise, the upper limits are $\mathcal{O}(10^{-1})$ - $\mathcal{O}(1)$.

6 Conclusions

In summary, we have searched for $B^0 \rightarrow A'A'$ decays for the first time using the full data set of $772 \times 10^6 B\bar{B}$ events of Belle. We restrict our study to the case where A' decays promptly to e^+e^- , $\mu^+\mu^-$, or hadronic final states, and consider five final states of B^0 which are $e^+e^-e^+e^-$, $e^+e^-\mu^+\mu^-$, $\mu^+\mu^-\mu^+\mu^-$, $e^+e^-\pi^+\pi^-$, and $\mu^+\mu^-\pi^+\pi^-$. From the branching fraction of A' , the five B^0 final states are merged to determine the branching fraction of $B^0 \rightarrow A'A'$. We find no significant signal in any assumed A' mass and decay mode, so we determine upper limits on $\mathcal{B}(B^0 \rightarrow A'A') \times \mathcal{B}(A' \rightarrow e^+e^-)^2$, $\mathcal{B}(B^0 \rightarrow A'A') \times \mathcal{B}(A' \rightarrow \mu^+\mu^-)^2$ and $\mathcal{B}(B^0 \rightarrow A'A')$, each at 90% C.L. The limits on the products of branching

¹B. Batell, private communication on the numerical factor of Eq. (5.1) of Ref. [5], when we apply B^0 -meson-related variables instead of B_s -meson and the measured Higgs mass.

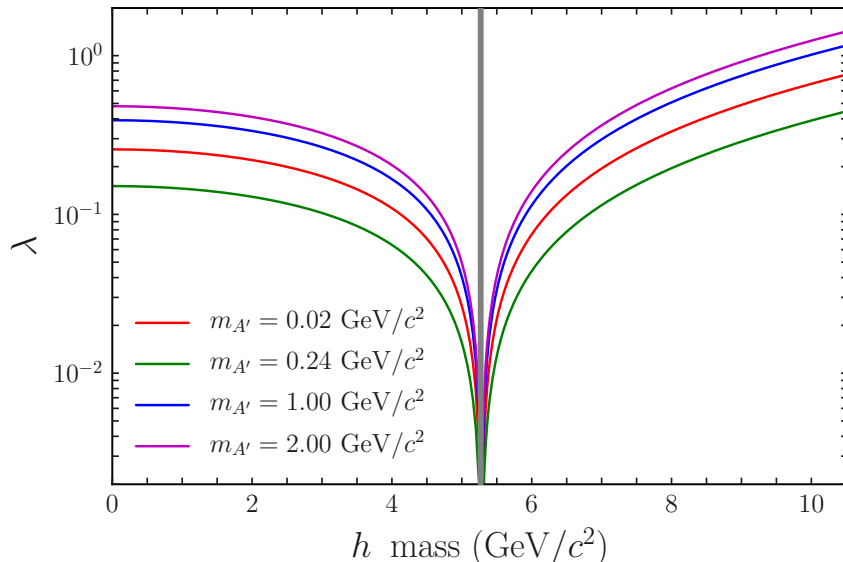


Figure 7. 90% upper limits of the Higgs portal coupling (λ) versus the dark Higgs mass for the 0.02, 0.24, 1.00, 2.00 GeV/c^2 dark photon.

fractions are of the order of $\mathcal{O}(10^{-8})$, while the limits on $\mathcal{B}(B^0 \rightarrow A'A')$ are $\mathcal{O}(10^{-8})$ – $\mathcal{O}(10^{-5})$. We also set 90% C.L. upper limits on the Higgs portal coupling λ for each assumed value of $m_{A'}$ and $m_{h'}$. The upper limits on λ are of the order of 10^{-2} – 10^{-1} at $m_{h'} \simeq m_{B^0} \pm 40 \text{ MeV}/c^2$ and 10^{-1} – 1 at $m_{h'} \simeq m_{B^0} \pm 3 \text{ GeV}/c^2$. With minor modifications our analysis can be used to set limits on the other new physics models which include prompt $B^0 \rightarrow XX$ and $X \rightarrow \ell^+\ell^-/\pi^+\pi^-$ decays. We expect to have much more stringent results from the Belle II experiment [40, 41], with nearly two orders of magnitude increase in statistics, in the future.

Acknowledgments

We thank B. Batell and M. Pospelov for the discussion of the $B^0 \rightarrow A'A'$ branching fraction which helped to finalize this paper. We thank the KEKB group for the excellent operation of the accelerator; the KEK cryogenics group for the efficient operation of the solenoid; and the KEK computer group, and the Pacific Northwest National Laboratory (PNNL) Environmental Molecular Sciences Laboratory (EMSL) computing group for strong computing support; and the National Institute of Informatics, and Science Information NETwork 5 (SINET5) for valuable network support. We acknowledge support from the Ministry of Education, Culture, Sports, Science, and Technology (MEXT) of Japan, the Japan Society for the Promotion of Science (JSPS), and the Tau-Lepton Physics Research Center of Nagoya University; the Australian Research Council including grants DP180102629, DP170102389, DP170102204, DP150103061, FT130100303; Austrian Federal Ministry of Education, Science and Research (FWF) and FWF Austrian Science

Fund No. P 31361-N36; the National Natural Science Foundation of China under Contracts No. 11435013, No. 11475187, No. 11521505, No. 11575017, No. 11675166, No. 11705209; Key Research Program of Frontier Sciences, Chinese Academy of Sciences (CAS), Grant No. QYZDJ-SSW-SLH011; the CAS Center for Excellence in Particle Physics (CCEPP); the Shanghai Pujiang Program under Grant No. 18PJ1401000; the Ministry of Education, Youth and Sports of the Czech Republic under Contract No. LTT17020; Horizon 2020 ERC Advanced Grant No. 884719 and ERC Starting Grant No. 947006 “InterLeptons” (European Union); the Carl Zeiss Foundation, the Deutsche Forschungsgemeinschaft, the Excellence Cluster Universe, and the VolkswagenStiftung; the Department of Atomic Energy (Project Identification No. RTI 4002) and the Department of Science and Technology of India; the Istituto Nazionale di Fisica Nucleare of Italy; National Research Foundation (NRF) of Korea Grant Nos. 2016R1D1A1B01010135, 2016R1D1A1B02012900, 2018R1A2B-3003643, 2018R1A6A1A06024970, 2018R1D1A1B07047294, 2018R1A4A1025334, 2019K1-A3A7A09033840, 2019K1A3A7A09034999, 2019R1I1A3A01058933; Radiation Science Research Institute, Foreign Large-size Research Facility Application Supporting project, the Global Science Experimental Data Hub Center of the Korea Institute of Science and Technology Information and KREONET/GLORIAD; the Polish Ministry of Science and Higher Education and the National Science Center; the Ministry of Science and Higher Education of the Russian Federation, Agreement 14.W03.31.0026, and the HSE University Basic Research Program, Moscow; University of Tabuk research grants S-1440-0321, S-0256-1438, and S-0280-1439 (Saudi Arabia); the Slovenian Research Agency Grant Nos. J1-9124 and P1-0135; Ikerbasque, Basque Foundation for Science, Spain; the Swiss National Science Foundation; the Ministry of Education and the Ministry of Science and Technology of Taiwan; and the United States Department of Energy and the National Science Foundation.

References

- [1] P. A. Zyla *et al.* (Particle Data Group), *The Review of Particle Physics*, PTEP **2020** (2020) 083C01.
- [2] Q. R. Ahmad *et al.* (SNO Collaboration), *Measurement of the Rate of $\nu_e + d \rightarrow p + p + e^-$ Interactions Produced by ^8B Solar Neutrinos at the Sudbury Neutrino Observatory*, Phys. Rev. Lett. **87** (2001) 071301.
- [3] Y. Fukuda *et al.* (Super-Kamiokande Collaboration), *Evidence for Oscillation of Atmospheric Neutrinos*, Phys. Rev. Lett. **81** (1998) 1562.
- [4] A. D. Sakharov, *Violation of CP Invariance, C asymmetry, and baryon asymmetry of the universe*, Sov. Phys. Usp. **34** (1991) 392.
- [5] B. Batell, M. Pospelov and A. Ritz, *Multi-lepton Signatures of a Hidden Sector in Rare B Decays*, Phys. Rev. D **83** (2011) 054005 [arXiv:0911.4938].
- [6] B. Holdom, *Two $U(1)$'s and ϵ Charge Shifts*, Phys. Lett. B **166** (1986) 196.
- [7] P. Fayet, *Effects of the Spin 1 Partner of the Goldstino (Gravitino) on Neutral Current Phenomenology*, Phys. Lett. B **95** (1980) 285.
- [8] P. Fayet, *On the Search for a New Spin 1 Boson*, Nucl. Phys. B **187** (1981) 184.

- [9] G. W. Bennett *et al.* (Muon g-2 Collaboration), *Final Report of the Muon E821 Anomalous Magnetic Moment Measurement at BNL*, Phys. Rev. D **73** (2006) 072003 [arXiv:hep-ex/0602035].
- [10] M. Pospelov, *Secluded U(1) below the weak scale*, Phys. Rev. D **80** (2009) 095002 [arXiv:0811.1030].
- [11] D. Tucker-Smith and I. Yavin, *Muonic hydrogen and MeV forces*, Phys. Rev. D **83** (2011) 101702 [arXiv:1011.4922].
- [12] B. Batell, D. McKeen and M. Pospelov, *New Parity-Violating Muonic Forces and the Proton Charge Radius*, Phys. Rev. Lett. **107** (2011) 011803 [arXiv:1103.0721].
- [13] N. Haba and S. Matsumoto, *Baryogenesis from Dark Sector*, Prog. Theor. Phys. **125** (2011) 1311 [arXiv:1008.2487].
- [14] J. Chang *et al.*, *An excess of cosmic ray electrons at energies of 300-800 GeV*, Nature **456** (2008) 362.
- [15] O. Adriani *et al.* (PAMELA Collaboration), *Cosmic-Ray Positron Energy Spectrum Measured by PAMELA*, Phys. Rev. Lett. **111** (2013) 081102 [arXiv:1308.0133].
- [16] M. Ackermann *et al.* (Fermi-LAT Collaboration), *Measurement of separate cosmic-ray electron and positron spectra with the Fermi Large Area Telescope*, Phys. Rev. Lett. **108** (2012) 011103 [arXiv:1109.0521].
- [17] M. Aguilar *et al.* (AMS Collaboration), *Electron and Positron Fluxes in Primary Cosmic Rays Measured with the Alpha Magnetic Spectrometer on the International Space Station*, Phys. Rev. Lett. **113** (2014) 121102.
- [18] C. R. Chen, F. Takahashi and T. T. Yanagida, *High-energy Cosmic-Ray Positrons from Hidden-Gauge-Boson Dark Matter*, Phys. Lett. B **673** (2009) 255 [arXiv:0811.0477].
- [19] C. Y. Chen, H. Davoudiasl, W. J. Marciano and C. Zhang, *Implications of a light "dark Higgs" solution to the $g_\mu - 2$ discrepancy*, Phys. Rev. D **93** (2016) 035006 [arXiv:1511.04715].
- [20] G. Arcadi *et al.*, *Lepton Flavor Violation Induced by Dark Matter*, Phys. Rev. D **97** (2018) 075022 [arXiv:1712.02373].
- [21] B. Batell, M. Pospelov and A. Ritz, *Probing a Secluded U(1) at B-factories*, Phys. Rev. D **79** (2009) 115008 [arXiv:0903.0363].
- [22] J. P. Lees *et al.* (BaBar Collaboration), *Search for Low-Mass Dark-Sector Higgs Bosons*, Phys. Rev. Lett. **108** (2012) 211801 [arXiv:1202.1313].
- [23] A. V. Danilina and N. V. Nikitin, *Four-Leptonic Decays of Charged and Neutral B Mesons within the Standard Model*, Phys. Atom. Nucl. **81** (2018) 347.
- [24] R. Aaij *et al.* (LHCb Collaboration), *Search for decays of neutral beauty mesons into four muons*, JHEP **03** (2017) 001 [arXiv:1611.07704].
- [25] R. Aaij *et al.* (LHCb Collaboration), *Study of the rare B_s^0 and B^0 decays into the $\pi^+\pi^-\mu^+\mu^-$ final state*, Phys. Lett. B **743** (2015) 46 [arXiv:1412.6433].
- [26] A. Abashian *et al.* (Belle Collaboration), *The Belle Detector*, Nucl. Instrum. Meth. A **479** (2002) 117.
- [27] J. Brodzicka *et al.* (Belle Collaboration), *Physics Achievements from the Belle Experiment*, PTEP **2012** (2012) 04D001 [arXiv:1212.5342].

- [28] S. Kurokawa and E. Kikutani, *Overview of the KEKB accelerators*, Nucl. Instrum. Meth. A **499** (2003) 1.
- [29] T. Abe *et al.*, *Achievements of KEKB*, PTEP **2013** (2013) 03A001.
- [30] D. J. Lange, *The EvtGen particle decay simulation package*, Nucl. Instrum. Methods Phys. Res., Sect. A **462** (2001) 152.
- [31] R. Brun, F. Bruyant, M. Maire, A. C. McPherson and P. Zancarini, *Geant3*, CERN-DD-EE-84-1.
- [32] A. Abashian, K. Abe, K. Abe, P. K. Behera, F. Handa, T. Iijima, Y. Inoue, H. Miyake, T. Nagamine and E. Nakano, *et al. Muon identification in the Belle experiment at KEKB*, Nucl. Instrum. Meth. A **491** (2002), 69-82.
- [33] K. Hanagaki, H. Kakuno, H. Ikeda, T. Iijima and T. Tsukamoto, *Electron identification in Belle*, Nucl. Instrum. Meth. A **485** (2002), 490-503 [arXiv:hep-ex/0108044].
- [34] E. Nakano, *Belle PID*, Nucl. Instrum. Meth. A **494** (2002), 402-408.
- [35] R. A. Fisher, *The use of multiple measurements in taxonomic problems*, Annals Eugen. **7** (1936) 179.
- [36] H. Voss, A. Hocker, J. Stelzer and F. Tegenfeldt, *TMVA - Toolkit for Multivariate Data Analysis*, PoS ACAT (2007) 040 [arXiv:physics/0703039].
- [37] S. H. Lee *et al.* (Belle Collaboration), *Evidence for $B^0 \rightarrow \pi^0 \pi^0$* , Phys. Rev. Lett. **91** (2003) 261801 [arXiv:hep-ex/0308040].
- [38] J. Conrad, O. Botner, A. Hallgren and C. Perez de los Heros, *Including systematic uncertainties in confidence interval construction for Poisson statistics*, Phys. Rev. D **67** (2003) 012002 [arXiv:hep-ex/0202013].
- [39] G. J. Feldman and R. D. Cousins, *A Unified approach to the classical statistical analysis of small signals*, Phys. Rev. D **57** (1998) 3873 [arXiv:physics/9711021].
- [40] T. Abe *et al.* (Belle II Collaboration), *Belle II Technical Design Report*, [arXiv:1011.0352].
- [41] E. Kou *et al.* (Belle II Collaboration), *The Belle II Physics Book*, PTEP **2019** (2019) 123C01 [arXiv:1808.10567].

1 Tables of signal efficiency, the number of expected background events, and the number of observed events at Belle

In this section, tables of signal efficiency (ϵ) in signal MC, the number of expected background events (N_{bkg}) in Belle background MC, and the number of observed events (N_{obs}) in the Belle data are introduced. The dark photon masses are in the range of ($m_{A'}$) in $0.01 - 2.62 \text{ GeV}/c^2$ with $10 \text{ MeV}/c^2$ ($0.01 - 1.10 \text{ GeV}/c^2$) and $20 \text{ MeV}/c^2$ ($1.10 - 2.62 \text{ GeV}/c^2$) intervals for $e^+e^-e^+e^-$, $e^+e^-\mu^+\mu^-$, $\mu^+\mu^-\mu^+\mu^-$, $e^+e^-\pi^+\pi^-$, $\mu^+\mu^-\pi^+\pi^-$ final states and $B^0 \rightarrow A'A'$ combined results.

For the combined signal efficiencies, we first obtain the ratio $F_f \equiv \mathcal{B}(B^0 \rightarrow A'A' \rightarrow f)/\mathcal{B}(B^0 \rightarrow A'A')$, where f is each final state, using the dark photon branching fraction. The dark photon branching fraction below the $\tau^+\tau^-$ threshold is obtained as

$$\mathcal{B}(A' \rightarrow \ell^+\ell^-/\pi^+\pi^-) = \frac{\Gamma_{A' \rightarrow \ell^+\ell^-/\pi^+\pi^-}}{\Gamma_{A' \rightarrow e^+e^-} + \Gamma_{A' \rightarrow \mu^+\mu^-} + \Gamma_{A' \rightarrow \text{hadrons}}}, \quad (1.1)$$

where $\ell = e$ or μ . Following Ref. [2], we write down the partial widths to $\ell^+\ell^-$ and hadrons as

$$\begin{aligned} \Gamma_{A' \rightarrow \ell^+\ell^-} &= \frac{1}{3} \alpha \epsilon_{\text{mixing}}^2 m_{A'} \sqrt{1 - 4m_\ell^2/m_{A'}^2} (1 + 2m_\ell^2/m_{A'}^2), \\ \Gamma_{A' \rightarrow \text{hadrons}} &= \Gamma_{A' \rightarrow \mu^+\mu^-} \times R(s = m_{A'}^2), \end{aligned} \quad (1.2)$$

with the square of the total center-of-mass (CM) frame energy s , the kinetic mixing parameter ϵ_{mix} , and $R(s) = \sigma_{e^+e^- \rightarrow \text{hadrons}}/\sigma_{e^+e^- \rightarrow \mu^+\mu^-}$ which is determined by various experiments [1]. The branching fraction of $A' \rightarrow \pi^+\pi^-$ is then obtained as [3]:

$$\mathcal{B}(A' \rightarrow \pi^+\pi^-) = \mathcal{B}(A' \rightarrow \text{hadrons}) \times \sigma(e^+e^- \rightarrow \pi^+\pi^-)/\sigma(e^+e^- \rightarrow \text{hadrons}). \quad (1.3)$$

From the A' branching fraction, we calculate F_f for each final state. In case of $e^+e^-\mu^+\mu^-$, for example, $F_{e^+e^-\mu^+\mu^-}$ is $2 \times \mathcal{B}(A' \rightarrow e^+e^-) \times \mathcal{B}(A' \rightarrow \mu^+\mu^-)$. With this ratio F_f , the combined efficiency is determined as $\sum_f \epsilon_f F_f$ where ϵ_f is the signal efficiency of the final state f .

Table 1: Signal efficiency (ϵ), the number of expected background events (N_{bkg}), and the number of observed events (N_{obs}) for $B^0 \rightarrow A'A' \rightarrow e^+e^-e^+e^-$ mode.

$m_{A'}$ (GeV/ c^2)	ϵ (%)	N_{bkg}	N_{obs}	$m_{A'}$ (GeV/ c^2)	ϵ (%)	N_{bkg}	N_{obs}
0.01	14.56 ± 1.34	0.33 ± 0.24	1	0.94	11.27 ± 1.04	0.00 ± 0.17	0
0.02	14.82 ± 1.36	0.83 ± 0.37	2	0.95	11.31 ± 1.05	0.00 ± 0.17	0
0.03	14.72 ± 1.35	0.50 ± 0.29	1	0.96	11.34 ± 1.05	0.00 ± 0.17	0
0.04	14.62 ± 1.33	0.00 ± 0.17	1	0.97	11.33 ± 1.05	0.00 ± 0.17	0
0.05	14.51 ± 1.32	0.00 ± 0.17	1	0.98	11.32 ± 1.05	0.00 ± 0.17	0
0.06	14.40 ± 1.31	0.00 ± 0.17	0	0.99	11.29 ± 1.05	0.00 ± 0.17	0
0.07	14.24 ± 1.30	0.00 ± 0.17	1	1.00	11.26 ± 1.05	0.00 ± 0.17	0
0.08	14.08 ± 1.28	0.00 ± 0.17	1	1.01	11.26 ± 1.05	0.00 ± 0.17	0
0.09	13.86 ± 1.26	0.00 ± 0.17	0	1.02	11.27 ± 1.05	0.00 ± 0.17	0
0.10	13.64 ± 1.24	0.00 ± 0.17	0	1.03	11.25 ± 1.05	0.00 ± 0.17	0
0.11	13.65 ± 1.24	0.00 ± 0.17	0	1.04	11.24 ± 1.05	0.00 ± 0.17	0
0.12	13.66 ± 1.24	0.00 ± 0.17	0	1.05	11.20 ± 1.05	0.00 ± 0.17	0
0.13	13.76 ± 1.25	0.00 ± 0.17	0	1.06	11.17 ± 1.05	0.00 ± 0.17	0
0.14	13.85 ± 1.26	0.00 ± 0.17	0	1.07	11.18 ± 1.05	0.00 ± 0.17	0

0.15	13.71 ± 1.25	0.00 ± 0.17	0	1.08	11.18 ± 1.05	0.00 ± 0.17	0
0.16	13.57 ± 1.24	0.00 ± 0.17	0	1.09	11.14 ± 1.04	0.00 ± 0.17	0
0.17	13.47 ± 1.23	0.00 ± 0.17	0	1.10	11.10 ± 1.04	0.00 ± 0.17	0
0.18	13.37 ± 1.22	0.00 ± 0.17	0	1.12	11.11 ± 1.04	0.00 ± 0.17	0
0.19	13.31 ± 1.21	0.00 ± 0.17	0	1.14	11.06 ± 1.04	0.00 ± 0.17	0
0.20	13.25 ± 1.21	0.00 ± 0.17	0	1.16	11.07 ± 1.04	0.00 ± 0.17	0
0.21	13.22 ± 1.20	0.00 ± 0.17	0	1.18	11.06 ± 1.05	0.00 ± 0.17	0
0.22	13.19 ± 1.20	0.00 ± 0.17	0	1.20	11.07 ± 1.05	0.00 ± 0.17	0
0.23	13.08 ± 1.19	0.00 ± 0.17	0	1.22	11.11 ± 1.06	0.00 ± 0.17	0
0.24	12.97 ± 1.18	0.00 ± 0.17	0	1.24	11.05 ± 1.05	0.00 ± 0.17	0
0.25	12.97 ± 1.18	0.00 ± 0.17	0	1.26	11.13 ± 1.06	0.00 ± 0.17	0
0.26	12.97 ± 1.18	0.00 ± 0.17	0	1.28	11.14 ± 1.07	0.00 ± 0.17	0
0.27	12.94 ± 1.17	0.00 ± 0.17	0	1.30	11.22 ± 1.08	0.00 ± 0.17	0
0.28	12.90 ± 1.17	0.00 ± 0.17	0	1.32	11.26 ± 1.08	0.00 ± 0.17	0
0.29	12.84 ± 1.16	0.00 ± 0.17	0	1.34	11.27 ± 1.09	0.00 ± 0.17	0
0.30	12.78 ± 1.16	0.00 ± 0.17	0	1.36	11.36 ± 1.09	0.00 ± 0.17	0
0.31	12.73 ± 1.15	0.00 ± 0.17	0	1.38	11.42 ± 1.10	0.00 ± 0.17	0
0.32	12.69 ± 1.15	0.00 ± 0.17	0	1.40	11.48 ± 1.11	0.00 ± 0.17	0
0.33	12.64 ± 1.15	0.00 ± 0.17	0	1.42	11.58 ± 1.12	0.00 ± 0.17	0
0.34	12.58 ± 1.14	0.00 ± 0.17	0	1.44	11.57 ± 1.12	0.00 ± 0.17	0
0.35	12.54 ± 1.14	0.00 ± 0.17	0	1.46	11.66 ± 1.13	0.00 ± 0.17	0
0.36	12.50 ± 1.13	0.00 ± 0.17	0	1.48	11.73 ± 1.13	0.00 ± 0.17	0
0.37	12.47 ± 1.13	0.00 ± 0.17	0	1.50	11.75 ± 1.14	0.00 ± 0.17	0
0.38	12.45 ± 1.13	0.00 ± 0.17	0	1.52	11.86 ± 1.15	0.00 ± 0.17	0
0.39	12.40 ± 1.12	0.00 ± 0.17	0	1.54	11.93 ± 1.15	0.00 ± 0.17	0
0.40	12.35 ± 1.12	0.00 ± 0.17	0	1.56	12.07 ± 1.17	0.00 ± 0.17	0
0.41	12.29 ± 1.11	0.00 ± 0.17	0	1.58	12.05 ± 1.16	0.00 ± 0.17	0
0.42	12.24 ± 1.11	0.00 ± 0.17	0	1.60	12.13 ± 1.17	0.00 ± 0.17	0
0.43	12.22 ± 1.11	0.00 ± 0.17	0	1.62	12.11 ± 1.17	0.00 ± 0.17	0
0.44	12.20 ± 1.11	0.00 ± 0.17	0	1.64	12.18 ± 1.18	0.00 ± 0.17	0
0.45	12.12 ± 1.10	0.00 ± 0.17	0	1.66	12.23 ± 1.18	0.00 ± 0.17	0
0.46	12.05 ± 1.09	0.00 ± 0.17	0	1.68	12.31 ± 1.19	0.00 ± 0.17	0
0.47	11.94 ± 1.08	0.00 ± 0.17	0	1.70	12.34 ± 1.19	0.00 ± 0.17	0
0.48	11.83 ± 1.08	0.00 ± 0.17	0	1.72	12.46 ± 1.21	0.00 ± 0.17	0
0.49	11.75 ± 1.07	0.00 ± 0.17	0	1.74	12.47 ± 1.21	0.00 ± 0.17	0
0.50	11.67 ± 1.06	0.00 ± 0.17	0	1.76	12.51 ± 1.21	0.00 ± 0.17	0
0.51	11.55 ± 1.05	0.00 ± 0.17	0	1.78	12.59 ± 1.21	0.00 ± 0.17	0
0.52	11.42 ± 1.04	0.00 ± 0.17	0	1.80	12.69 ± 1.22	0.00 ± 0.17	0
0.53	11.34 ± 1.03	0.00 ± 0.17	0	1.82	12.79 ± 1.23	0.00 ± 0.17	0
0.54	11.26 ± 1.03	0.00 ± 0.17	0	1.84	12.90 ± 1.24	0.00 ± 0.17	0
0.55	11.19 ± 1.02	0.00 ± 0.17	0	1.86	12.93 ± 1.24	0.00 ± 0.17	0
0.56	11.11 ± 1.01	0.00 ± 0.17	0	1.88	13.02 ± 1.25	0.00 ± 0.17	0
0.57	11.12 ± 1.02	0.00 ± 0.17	0	1.90	13.06 ± 1.25	0.10 ± 0.19	0
0.58	11.12 ± 1.02	0.00 ± 0.17	0	1.92	13.12 ± 1.26	0.10 ± 0.19	0
0.59	11.10 ± 1.02	0.10 ± 0.19	0	1.94	13.25 ± 1.27	0.10 ± 0.19	0
0.60	11.07 ± 1.01	0.10 ± 0.19	0	1.96	13.27 ± 1.27	0.10 ± 0.19	0
0.61	11.00 ± 1.01	0.10 ± 0.19	0	1.98	13.40 ± 1.28	0.25 ± 0.22	0
0.62	10.94 ± 1.00	0.10 ± 0.19	0	2.00	13.43 ± 1.28	0.25 ± 0.22	0
0.63	10.93 ± 1.00	0.10 ± 0.19	0	2.02	13.55 ± 1.29	0.25 ± 0.22	0

0.64	10.92 ± 1.00	0.10 ± 0.19	0	2.04	13.63 ± 1.30	0.15 ± 0.20	0
0.65	10.91 ± 1.00	0.00 ± 0.17	0	2.06	13.74 ± 1.30	0.15 ± 0.20	0
0.66	10.90 ± 1.00	0.00 ± 0.17	0	2.08	13.83 ± 1.31	0.15 ± 0.20	0
0.67	10.91 ± 1.00	0.00 ± 0.17	0	2.10	13.90 ± 1.31	0.15 ± 0.20	0
0.68	10.92 ± 1.00	0.00 ± 0.17	0	2.12	13.95 ± 1.31	0.15 ± 0.20	0
0.69	10.94 ± 1.00	0.00 ± 0.17	0	2.14	14.14 ± 1.33	0.20 ± 0.22	0
0.70	10.96 ± 1.01	0.00 ± 0.17	0	2.16	14.21 ± 1.33	0.20 ± 0.22	0
0.71	10.99 ± 1.01	0.00 ± 0.17	0	2.18	14.31 ± 1.34	0.20 ± 0.22	0
0.72	11.02 ± 1.02	0.00 ± 0.17	0	2.20	14.51 ± 1.36	0.20 ± 0.22	0
0.73	11.07 ± 1.02	0.00 ± 0.17	0	2.22	14.63 ± 1.36	0.20 ± 0.22	0
0.74	11.12 ± 1.02	0.00 ± 0.17	0	2.24	14.79 ± 1.38	0.20 ± 0.22	0
0.75	11.19 ± 1.03	0.00 ± 0.17	0	2.26	14.98 ± 1.38	0.20 ± 0.22	0
0.76	11.26 ± 1.04	0.00 ± 0.17	0	2.28	15.09 ± 1.39	0.10 ± 0.19	0
0.77	11.33 ± 1.04	0.00 ± 0.17	0	2.30	15.32 ± 1.41	0.00 ± 0.17	0
0.78	11.39 ± 1.05	0.00 ± 0.17	0	2.32	15.52 ± 1.42	0.00 ± 0.17	0
0.79	11.39 ± 1.05	0.00 ± 0.17	0	2.34	15.77 ± 1.44	0.10 ± 0.19	0
0.80	11.40 ± 1.05	0.00 ± 0.17	0	2.36	15.99 ± 1.45	0.20 ± 0.22	0
0.81	11.41 ± 1.05	0.00 ± 0.17	0	2.38	16.25 ± 1.47	0.20 ± 0.22	0
0.82	11.42 ± 1.05	0.00 ± 0.17	0	2.40	16.47 ± 1.48	0.20 ± 0.22	0
0.83	11.45 ± 1.06	0.00 ± 0.17	0	2.42	16.79 ± 1.50	0.20 ± 0.22	0
0.84	11.49 ± 1.06	0.00 ± 0.17	0	2.44	16.88 ± 1.50	0.20 ± 0.22	0
0.85	11.52 ± 1.06	0.00 ± 0.17	0	2.46	17.41 ± 1.54	0.20 ± 0.22	0
0.86	11.55 ± 1.06	0.00 ± 0.17	0	2.48	17.76 ± 1.56	0.20 ± 0.22	0
0.87	11.50 ± 1.06	0.00 ± 0.17	0	2.50	18.15 ± 1.58	0.20 ± 0.22	0
0.88	11.45 ± 1.06	0.00 ± 0.17	0	2.52	18.53 ± 1.60	0.00 ± 0.17	0
0.89	11.46 ± 1.06	0.00 ± 0.17	0	2.54	18.82 ± 1.61	0.00 ± 0.17	0
0.90	11.47 ± 1.06	0.00 ± 0.17	0	2.56	19.53 ± 1.64	0.00 ± 0.17	0
0.91	11.47 ± 1.06	0.00 ± 0.17	0	2.58	20.21 ± 1.65	0.00 ± 0.17	0
0.92	11.47 ± 1.06	0.00 ± 0.17	0	2.60	21.05 ± 1.67	0.00 ± 0.17	0
0.93	11.37 ± 1.05	0.00 ± 0.17	0	2.62	21.53 ± 1.64	0.00 ± 0.17	0

Table 2: Signal efficiency (ϵ), the number of expected background events (N_{bkg}), and the number of observed events (N_{obs}) for $B^0 \rightarrow A'A' \rightarrow e^+e^-\mu^+\mu^-$ mode.

$m_{A'}$ (GeV/ c^2)	ϵ (%)	N_{bkg}	N_{obs}	$m_{A'}$ (GeV/ c^2)	ϵ (%)	N_{bkg}	N_{obs}
0.22	23.93 ± 1.68	0.00 ± 0.17	0	1.05	9.89 ± 0.68	0.00 ± 0.17	0
0.23	22.79 ± 1.59	0.00 ± 0.17	0	1.06	9.99 ± 0.68	0.00 ± 0.17	0
0.24	21.65 ± 1.51	0.00 ± 0.17	0	1.07	9.99 ± 0.69	0.00 ± 0.17	0
0.25	20.06 ± 1.39	0.00 ± 0.17	0	1.08	9.98 ± 0.69	0.00 ± 0.17	0
0.26	18.46 ± 1.28	0.00 ± 0.17	0	1.09	9.95 ± 0.68	0.00 ± 0.17	0
0.27	17.35 ± 1.21	0.00 ± 0.17	0	1.10	9.91 ± 0.68	0.00 ± 0.17	0
0.28	16.25 ± 1.13	0.00 ± 0.17	0	1.12	9.95 ± 0.69	0.00 ± 0.17	0
0.29	15.63 ± 1.09	0.00 ± 0.17	0	1.14	9.94 ± 0.69	0.00 ± 0.17	0
0.30	15.01 ± 1.04	0.00 ± 0.17	0	1.16	9.92 ± 0.69	0.00 ± 0.17	0
0.31	14.63 ± 1.02	0.00 ± 0.17	0	1.18	9.93 ± 0.69	0.00 ± 0.17	0
0.32	14.26 ± 0.99	0.00 ± 0.17	0	1.20	9.88 ± 0.69	0.00 ± 0.17	0

0.33	13.92 ± 0.97	0.00 ± 0.17	0	1.22	10.03 ± 0.70	0.00 ± 0.17	0
0.34	13.58 ± 0.94	0.00 ± 0.17	0	1.24	9.96 ± 0.70	0.00 ± 0.17	0
0.35	13.33 ± 0.92	0.00 ± 0.17	0	1.26	10.01 ± 0.70	0.00 ± 0.17	0
0.36	13.07 ± 0.90	0.00 ± 0.17	0	1.28	10.05 ± 0.71	0.00 ± 0.17	0
0.37	12.88 ± 0.89	0.00 ± 0.17	0	1.30	10.11 ± 0.71	0.00 ± 0.17	0
0.38	12.70 ± 0.88	0.00 ± 0.17	0	1.32	10.08 ± 0.71	0.00 ± 0.17	0
0.39	12.57 ± 0.87	0.00 ± 0.17	0	1.34	10.09 ± 0.72	0.10 ± 0.19	0
0.40	12.44 ± 0.86	0.00 ± 0.17	0	1.36	10.09 ± 0.72	0.10 ± 0.19	0
0.41	12.30 ± 0.85	0.00 ± 0.17	0	1.38	10.12 ± 0.72	0.20 ± 0.22	0
0.42	12.15 ± 0.84	0.00 ± 0.17	0	1.40	10.18 ± 0.73	0.10 ± 0.19	0
0.43	12.05 ± 0.83	0.00 ± 0.17	0	1.42	10.24 ± 0.73	0.10 ± 0.19	0
0.44	11.95 ± 0.82	0.00 ± 0.17	0	1.44	10.27 ± 0.74	0.00 ± 0.17	0
0.45	11.85 ± 0.82	0.00 ± 0.17	0	1.46	10.31 ± 0.74	0.00 ± 0.17	0
0.46	11.75 ± 0.81	0.00 ± 0.17	0	1.48	10.12 ± 0.73	0.00 ± 0.17	0
0.47	11.67 ± 0.80	0.00 ± 0.17	0	1.50	10.37 ± 0.75	0.00 ± 0.17	0
0.48	11.60 ± 0.80	0.00 ± 0.17	0	1.52	10.37 ± 0.75	0.00 ± 0.17	0
0.49	11.50 ± 0.79	0.00 ± 0.17	0	1.54	10.44 ± 0.76	0.00 ± 0.17	0
0.50	11.39 ± 0.78	0.00 ± 0.17	0	1.56	10.47 ± 0.76	0.00 ± 0.17	0
0.51	11.25 ± 0.77	0.00 ± 0.17	0	1.58	10.53 ± 0.77	0.00 ± 0.17	0
0.52	11.12 ± 0.76	0.00 ± 0.17	0	1.60	10.57 ± 0.77	0.00 ± 0.17	0
0.53	11.05 ± 0.76	0.00 ± 0.17	0	1.62	10.66 ± 0.78	0.00 ± 0.17	0
0.54	10.98 ± 0.75	0.00 ± 0.17	0	1.64	10.74 ± 0.79	0.00 ± 0.17	0
0.55	10.92 ± 0.75	0.00 ± 0.17	0	1.66	10.74 ± 0.79	0.00 ± 0.17	0
0.56	10.87 ± 0.74	0.00 ± 0.17	0	1.68	10.88 ± 0.81	0.00 ± 0.17	0
0.57	10.80 ± 0.74	0.00 ± 0.17	0	1.70	10.86 ± 0.81	0.00 ± 0.17	0
0.58	10.74 ± 0.73	0.00 ± 0.17	0	1.72	11.04 ± 0.82	0.00 ± 0.17	0
0.59	10.73 ± 0.73	0.00 ± 0.17	0	1.74	11.13 ± 0.83	0.00 ± 0.17	0
0.60	10.71 ± 0.73	0.00 ± 0.17	0	1.76	11.13 ± 0.83	0.00 ± 0.17	0
0.61	10.70 ± 0.73	0.00 ± 0.17	0	1.78	11.33 ± 0.85	0.00 ± 0.17	0
0.62	10.68 ± 0.73	0.00 ± 0.17	0	1.80	11.42 ± 0.85	0.00 ± 0.17	0
0.63	10.64 ± 0.73	0.00 ± 0.17	0	1.82	11.58 ± 0.87	0.00 ± 0.17	0
0.64	10.59 ± 0.72	0.00 ± 0.17	0	1.84	11.62 ± 0.87	0.00 ± 0.17	0
0.65	10.58 ± 0.72	0.00 ± 0.17	0	1.86	11.87 ± 0.89	0.00 ± 0.17	0
0.66	10.57 ± 0.72	0.00 ± 0.17	0	1.88	11.93 ± 0.89	0.00 ± 0.17	0
0.67	10.51 ± 0.72	0.00 ± 0.17	0	1.90	12.02 ± 0.90	0.00 ± 0.17	0
0.68	10.45 ± 0.71	0.00 ± 0.17	0	1.92	12.29 ± 0.92	0.00 ± 0.17	0
0.69	10.46 ± 0.71	0.00 ± 0.17	0	1.94	12.43 ± 0.93	0.00 ± 0.17	0
0.70	10.46 ± 0.71	0.00 ± 0.17	0	1.96	12.67 ± 0.95	0.00 ± 0.17	0
0.71	10.48 ± 0.71	0.00 ± 0.17	0	1.98	12.81 ± 0.96	0.00 ± 0.17	0
0.72	10.49 ± 0.71	0.00 ± 0.17	0	2.00	13.08 ± 0.97	0.00 ± 0.17	0
0.73	10.49 ± 0.71	0.00 ± 0.17	0	2.02	13.20 ± 0.98	0.10 ± 0.19	0
0.74	10.48 ± 0.71	0.00 ± 0.17	0	2.04	13.48 ± 1.00	0.10 ± 0.19	0
0.75	10.53 ± 0.71	0.00 ± 0.17	0	2.06	13.76 ± 1.02	0.10 ± 0.19	0
0.76	10.59 ± 0.72	0.00 ± 0.17	0	2.08	14.01 ± 1.03	0.00 ± 0.17	0
0.77	10.57 ± 0.72	0.00 ± 0.17	0	2.10	14.39 ± 1.05	0.00 ± 0.17	0
0.78	10.55 ± 0.72	0.00 ± 0.17	0	2.12	14.55 ± 1.06	0.00 ± 0.17	0
0.79	10.55 ± 0.72	0.00 ± 0.17	0	2.14	15.07 ± 1.09	0.00 ± 0.17	0
0.80	10.54 ± 0.72	0.00 ± 0.17	0	2.16	15.44 ± 1.12	0.00 ± 0.17	0
0.81	10.53 ± 0.71	0.00 ± 0.17	0	2.18	15.79 ± 1.13	0.10 ± 0.19	0

0.82	10.51 ± 0.71	0.00 ± 0.17	0	2.20	16.20 ± 1.16	0.10 ± 0.19	0
0.83	10.53 ± 0.71	0.00 ± 0.17	0	2.22	16.68 ± 1.18	0.10 ± 0.19	0
0.84	10.55 ± 0.72	0.00 ± 0.17	0	2.24	17.13 ± 1.21	0.10 ± 0.19	0
0.85	10.53 ± 0.71	0.00 ± 0.17	0	2.26	17.60 ± 1.23	0.00 ± 0.17	0
0.86	10.51 ± 0.71	0.00 ± 0.17	0	2.28	18.10 ± 1.26	0.10 ± 0.19	0
0.87	10.52 ± 0.71	0.00 ± 0.17	0	2.30	18.47 ± 1.28	0.10 ± 0.19	0
0.88	10.54 ± 0.71	0.00 ± 0.17	0	2.32	18.91 ± 1.30	0.10 ± 0.19	0
0.89	10.49 ± 0.71	0.00 ± 0.17	0	2.34	19.36 ± 1.33	0.10 ± 0.19	0
0.90	10.45 ± 0.71	0.00 ± 0.17	0	2.36	19.90 ± 1.36	0.00 ± 0.17	0
0.91	10.44 ± 0.71	0.00 ± 0.17	0	2.38	20.28 ± 1.38	0.00 ± 0.17	0
0.92	10.42 ± 0.71	0.10 ± 0.19	0	2.40	20.79 ± 1.41	0.00 ± 0.17	0
0.93	10.39 ± 0.70	0.10 ± 0.19	0	2.42	21.24 ± 1.44	0.00 ± 0.17	0
0.94	10.35 ± 0.70	0.10 ± 0.19	0	2.44	21.73 ± 1.46	0.00 ± 0.17	0
0.95	10.33 ± 0.70	0.10 ± 0.19	0	2.46	22.17 ± 1.49	0.00 ± 0.17	0
0.96	10.32 ± 0.70	0.00 ± 0.17	0	2.48	22.77 ± 1.52	0.00 ± 0.17	0
0.97	10.26 ± 0.70	0.00 ± 0.17	0	2.50	23.24 ± 1.55	0.00 ± 0.17	0
0.98	10.20 ± 0.69	0.00 ± 0.17	0	2.52	23.82 ± 1.58	0.00 ± 0.17	0
0.99	10.20 ± 0.69	0.00 ± 0.17	0	2.54	24.41 ± 1.61	0.00 ± 0.17	0
1.00	10.20 ± 0.69	0.00 ± 0.17	0	2.56	25.01 ± 1.64	0.00 ± 0.17	0
1.01	10.16 ± 0.69	0.00 ± 0.17	0	2.58	25.69 ± 1.66	0.10 ± 0.19	0
1.02	10.13 ± 0.69	0.00 ± 0.17	0	2.60	26.34 ± 1.68	0.10 ± 0.19	0
1.03	9.96 ± 0.68	0.00 ± 0.17	0	2.62	26.97 ± 1.69	0.10 ± 0.19	0
1.04	9.80 ± 0.67	0.00 ± 0.17	0				

Table 3: Signal efficiency (ϵ), the number of expected background events (N_{bkg}), and the number of observed events (N_{obs}) for $B^0 \rightarrow A'A' \rightarrow \mu^+\mu^-\mu^+\mu^-$ mode.

$m_{A'}$ (GeV/ c^2)	ϵ (%)	N_{bkg}	N_{obs}	$m_{A'}$ (GeV/ c^2)	ϵ (%)	N_{bkg}	N_{obs}
0.22	34.57 ± 2.86	0.00 ± 0.17	0	1.05	6.35 ± 0.52	0.00 ± 0.17	0
0.23	31.31 ± 2.54	0.00 ± 0.17	0	1.06	6.31 ± 0.52	0.00 ± 0.17	0
0.24	28.05 ± 2.23	0.00 ± 0.17	0	1.07	6.28 ± 0.51	0.00 ± 0.17	0
0.25	24.10 ± 1.91	0.00 ± 0.17	0	1.08	6.26 ± 0.51	0.00 ± 0.17	0
0.26	20.16 ± 1.60	0.00 ± 0.17	0	1.09	6.26 ± 0.52	0.00 ± 0.17	0
0.27	17.91 ± 1.42	0.00 ± 0.17	0	1.10	6.27 ± 0.52	0.00 ± 0.17	0
0.28	15.67 ± 1.25	0.00 ± 0.17	0	1.12	6.28 ± 0.52	0.00 ± 0.17	0
0.29	14.45 ± 1.15	0.00 ± 0.17	0	1.14	6.32 ± 0.53	0.00 ± 0.17	0
0.30	13.22 ± 1.05	0.00 ± 0.17	0	1.16	6.32 ± 0.53	0.00 ± 0.17	0
0.31	12.56 ± 1.00	0.00 ± 0.17	0	1.18	6.32 ± 0.53	0.00 ± 0.17	0
0.32	11.90 ± 0.95	0.00 ± 0.17	0	1.20	6.34 ± 0.54	0.00 ± 0.17	0
0.33	11.41 ± 0.91	0.00 ± 0.17	0	1.22	6.39 ± 0.54	0.00 ± 0.17	0
0.34	10.93 ± 0.87	0.00 ± 0.17	0	1.24	6.41 ± 0.55	0.00 ± 0.17	0
0.35	10.38 ± 0.82	0.00 ± 0.17	0	1.26	6.36 ± 0.54	0.00 ± 0.17	0
0.36	9.83 ± 0.78	0.00 ± 0.17	0	1.28	6.41 ± 0.55	0.00 ± 0.17	0
0.37	9.74 ± 0.77	0.00 ± 0.17	0	1.30	6.40 ± 0.55	0.00 ± 0.17	0
0.38	9.65 ± 0.77	0.00 ± 0.17	0	1.32	6.41 ± 0.56	0.00 ± 0.17	0
0.39	9.41 ± 0.75	0.00 ± 0.17	0	1.34	6.43 ± 0.56	0.00 ± 0.17	0

0.40	9.18 ± 0.73	0.00 ± 0.17	0	1.36	6.41 ± 0.56	0.00 ± 0.17	0
0.41	9.00 ± 0.71	0.00 ± 0.17	0	1.38	6.48 ± 0.57	0.00 ± 0.17	0
0.42	8.83 ± 0.70	0.00 ± 0.17	0	1.40	6.44 ± 0.57	0.00 ± 0.17	0
0.43	8.67 ± 0.69	0.00 ± 0.17	0	1.42	6.46 ± 0.57	0.00 ± 0.17	0
0.44	8.52 ± 0.68	0.00 ± 0.17	0	1.44	6.46 ± 0.58	0.00 ± 0.17	0
0.45	8.43 ± 0.67	0.00 ± 0.17	0	1.46	6.45 ± 0.58	0.00 ± 0.17	0
0.46	8.34 ± 0.66	0.00 ± 0.17	0	1.48	6.50 ± 0.59	0.00 ± 0.17	0
0.47	8.25 ± 0.65	0.00 ± 0.17	0	1.50	6.45 ± 0.59	0.00 ± 0.17	0
0.48	8.15 ± 0.65	0.00 ± 0.17	0	1.52	6.50 ± 0.59	0.00 ± 0.17	0
0.49	8.06 ± 0.64	0.00 ± 0.17	0	1.54	6.50 ± 0.60	0.00 ± 0.17	0
0.50	7.98 ± 0.63	0.00 ± 0.17	0	1.56	6.52 ± 0.60	0.00 ± 0.17	0
0.51	7.93 ± 0.63	0.00 ± 0.17	0	1.58	6.58 ± 0.61	0.00 ± 0.17	0
0.52	7.88 ± 0.62	0.00 ± 0.17	0	1.60	6.62 ± 0.62	0.00 ± 0.17	0
0.53	7.81 ± 0.62	0.00 ± 0.17	0	1.62	6.59 ± 0.62	0.00 ± 0.17	0
0.54	7.74 ± 0.61	0.00 ± 0.17	0	1.64	6.66 ± 0.63	0.00 ± 0.17	0
0.55	7.70 ± 0.61	0.00 ± 0.17	0	1.66	6.74 ± 0.64	0.00 ± 0.17	0
0.56	7.66 ± 0.60	0.00 ± 0.17	0	1.68	6.79 ± 0.65	0.00 ± 0.17	0
0.57	7.61 ± 0.60	0.00 ± 0.17	0	1.70	6.78 ± 0.66	0.00 ± 0.17	0
0.58	7.57 ± 0.60	0.00 ± 0.17	0	1.72	6.89 ± 0.67	0.00 ± 0.17	0
0.59	7.55 ± 0.60	0.00 ± 0.17	0	1.74	6.99 ± 0.68	0.00 ± 0.17	0
0.60	7.53 ± 0.59	0.00 ± 0.17	0	1.76	7.03 ± 0.69	0.00 ± 0.17	0
0.61	7.49 ± 0.59	0.00 ± 0.17	0	1.78	7.14 ± 0.70	0.00 ± 0.17	0
0.62	7.44 ± 0.59	0.00 ± 0.17	0	1.80	7.24 ± 0.71	0.00 ± 0.17	0
0.63	7.39 ± 0.58	0.00 ± 0.17	0	1.82	7.37 ± 0.73	0.00 ± 0.17	0
0.64	7.34 ± 0.58	0.00 ± 0.17	0	1.84	7.29 ± 0.72	0.00 ± 0.17	0
0.65	7.32 ± 0.58	0.00 ± 0.17	0	1.86	7.60 ± 0.76	0.00 ± 0.17	0
0.66	7.31 ± 0.58	0.00 ± 0.17	0	1.88	7.76 ± 0.77	0.00 ± 0.17	0
0.67	7.28 ± 0.57	0.00 ± 0.17	0	1.90	7.94 ± 0.79	0.00 ± 0.17	0
0.68	7.25 ± 0.57	0.00 ± 0.17	0	1.92	8.12 ± 0.81	0.00 ± 0.17	0
0.69	7.22 ± 0.57	0.00 ± 0.17	0	1.94	8.29 ± 0.83	0.00 ± 0.17	0
0.70	7.18 ± 0.57	0.00 ± 0.17	0	1.96	8.51 ± 0.85	0.00 ± 0.17	0
0.71	7.15 ± 0.56	0.00 ± 0.17	0	1.98	8.76 ± 0.87	0.00 ± 0.17	0
0.72	7.12 ± 0.56	0.00 ± 0.17	0	2.00	8.84 ± 0.88	0.00 ± 0.17	0
0.73	7.08 ± 0.56	0.00 ± 0.17	0	2.02	9.20 ± 0.91	0.00 ± 0.17	0
0.74	7.04 ± 0.55	0.00 ± 0.17	0	2.04	9.49 ± 0.94	0.00 ± 0.17	0
0.75	7.04 ± 0.55	0.00 ± 0.17	0	2.06	9.82 ± 0.97	0.00 ± 0.17	0
0.76	7.04 ± 0.55	0.00 ± 0.17	0	2.08	10.13 ± 1.00	0.00 ± 0.17	0
0.77	7.00 ± 0.55	0.00 ± 0.17	0	2.10	10.52 ± 1.03	0.00 ± 0.17	0
0.78	6.96 ± 0.55	0.00 ± 0.17	0	2.12	10.88 ± 1.05	0.00 ± 0.17	0
0.79	6.96 ± 0.55	0.00 ± 0.17	0	2.14	11.37 ± 1.09	0.00 ± 0.17	0
0.80	6.97 ± 0.55	0.00 ± 0.17	0	2.16	11.82 ± 1.13	0.00 ± 0.17	0
0.81	6.93 ± 0.55	0.00 ± 0.17	0	2.18	12.30 ± 1.16	0.00 ± 0.17	0
0.82	6.89 ± 0.54	0.00 ± 0.17	0	2.20	12.88 ± 1.21	0.00 ± 0.17	0
0.83	6.86 ± 0.54	0.00 ± 0.17	0	2.22	13.53 ± 1.26	0.00 ± 0.17	0
0.84	6.82 ± 0.54	0.00 ± 0.17	0	2.24	14.16 ± 1.31	0.00 ± 0.17	0
0.85	6.83 ± 0.54	0.00 ± 0.17	0	2.26	14.80 ± 1.35	0.00 ± 0.17	0
0.86	6.83 ± 0.54	0.00 ± 0.17	0	2.28	15.38 ± 1.39	0.00 ± 0.17	0
0.87	6.76 ± 0.54	0.00 ± 0.17	0	2.30	16.01 ± 1.44	0.00 ± 0.17	0
0.88	6.69 ± 0.53	0.00 ± 0.17	0	2.32	16.61 ± 1.48	0.00 ± 0.17	0

0.89	6.71 ± 0.53	0.00 ± 0.17	0	2.34	17.25 ± 1.53	0.00 ± 0.17	0
0.90	6.73 ± 0.54	0.00 ± 0.17	0	2.36	17.84 ± 1.58	0.00 ± 0.17	0
0.91	6.71 ± 0.53	0.00 ± 0.17	0	2.38	18.54 ± 1.63	0.00 ± 0.17	0
0.92	6.69 ± 0.53	0.00 ± 0.17	0	2.40	19.21 ± 1.68	0.00 ± 0.17	0
0.93	6.63 ± 0.53	0.00 ± 0.17	0	2.42	19.76 ± 1.73	0.00 ± 0.17	0
0.94	6.58 ± 0.52	0.00 ± 0.17	0	2.44	20.43 ± 1.78	0.00 ± 0.17	0
0.95	6.57 ± 0.52	0.00 ± 0.17	0	2.46	21.05 ± 1.84	0.00 ± 0.17	0
0.96	6.56 ± 0.53	0.00 ± 0.17	0	2.48	21.69 ± 1.89	0.00 ± 0.17	0
0.97	6.55 ± 0.53	0.00 ± 0.17	0	2.50	22.40 ± 1.95	0.00 ± 0.17	0
0.98	6.53 ± 0.52	0.00 ± 0.17	0	2.52	23.15 ± 2.02	0.00 ± 0.17	0
0.99	6.48 ± 0.52	0.00 ± 0.17	0	2.54	23.90 ± 2.09	0.00 ± 0.17	0
1.00	6.42 ± 0.52	0.00 ± 0.17	0	2.56	24.81 ± 2.17	0.00 ± 0.17	0
1.01	6.42 ± 0.52	0.00 ± 0.17	0	2.58	25.70 ± 2.24	0.00 ± 0.17	0
1.02	6.43 ± 0.52	0.00 ± 0.17	0	2.60	26.85 ± 2.34	0.00 ± 0.17	0
1.03	6.41 ± 0.52	0.00 ± 0.17	0	2.62	27.62 ± 2.40	0.00 ± 0.17	0
1.04	6.40 ± 0.52	0.00 ± 0.17	0				

Table 4: Signal efficiency (ϵ), the number of expected background events (N_{bkg}), and the number of observed events (N_{obs}) for $B^0 \rightarrow A'A' \rightarrow e^+e^-\pi^+\pi^-$ mode.

$m_{A'}$ (GeV/ c^2)	ϵ (%)	N_{bkg}	N_{obs}	$m_{A'}$ (GeV/ c^2)	ϵ (%)	N_{bkg}	N_{obs}
0.28	20.84 ± 1.25	0.00 ± 0.49	0	1.70	13.74 ± 0.82	0.40 ± 0.53	0
0.29	21.00 ± 1.25	0.50 ± 0.50	0	1.72	12.70 ± 0.76	0.30 ± 0.52	0
0.30	21.16 ± 1.26	0.00 ± 0.49	0	1.74	13.48 ± 0.81	0.20 ± 0.51	0
0.31	21.08 ± 1.25	0.00 ± 0.49	0	1.76	9.27 ± 0.55	0.30 ± 0.52	0
0.32	21.00 ± 1.24	0.00 ± 0.49	0	1.78	7.13 ± 0.43	0.40 ± 0.53	0
0.33	20.97 ± 1.24	0.00 ± 0.49	0	1.80	13.49 ± 0.82	0.40 ± 0.53	0
0.34	20.94 ± 1.24	0.00 ± 0.49	0	1.82	18.39 ± 1.10	0.60 ± 0.55	0
0.35	20.82 ± 1.23	0.00 ± 0.49	0	1.84	17.80 ± 1.07	0.90 ± 0.54	0
0.36	20.70 ± 1.23	0.00 ± 0.49	0	1.88	10.01 ± 0.60	1.30 ± 0.73	0
0.37	20.52 ± 1.22	0.00 ± 0.49	0	1.90	17.73 ± 1.06	0.50 ± 0.54	0
0.38	20.33 ± 1.21	0.00 ± 0.49	0	1.92	18.53 ± 1.11	0.85 ± 0.57	0
0.39	19.79 ± 1.18	0.50 ± 0.50	0	1.94	19.28 ± 1.15	1.05 ± 0.58	0
0.40	19.25 ± 1.15	0.50 ± 0.50	0	1.96	19.23 ± 1.15	0.97 ± 0.58	0
0.41	19.10 ± 1.15	0.50 ± 0.50	0	1.98	19.51 ± 1.16	1.52 ± 0.59	0
0.42	18.96 ± 1.14	0.00 ± 0.49	0	2.00	19.94 ± 1.19	1.32 ± 0.57	0
0.43	18.52 ± 1.11	0.00 ± 0.49	0	2.02	19.80 ± 1.17	1.39 ± 0.58	0
0.44	18.08 ± 1.09	0.50 ± 0.50	0	2.04	20.18 ± 1.20	1.57 ± 0.59	1
1.10	14.73 ± 0.87	0.30 ± 0.52	0	2.06	20.27 ± 1.20	1.32 ± 0.60	1
1.12	14.70 ± 0.87	0.24 ± 0.51	0	2.08	20.39 ± 1.21	0.95 ± 0.58	1
1.14	14.77 ± 0.88	0.64 ± 0.51	0	2.10	20.10 ± 1.19	0.75 ± 0.56	0
1.16	14.69 ± 0.87	0.62 ± 0.51	0	2.12	20.50 ± 1.21	1.80 ± 0.62	2
1.18	14.40 ± 0.86	0.85 ± 0.53	1	2.14	20.58 ± 1.21	1.60 ± 0.60	2
1.20	14.72 ± 0.88	0.25 ± 0.51	1	2.16	20.61 ± 1.21	2.00 ± 0.63	2
1.22	14.82 ± 0.88	0.20 ± 0.50	0	2.18	20.68 ± 1.21	1.60 ± 0.63	0
1.24	14.58 ± 0.87	0.25 ± 0.51	0	2.20	17.77 ± 1.04	1.30 ± 0.61	0

1.26	14.83 ± 0.88	0.75 ± 0.52	1	2.22	18.07 ± 1.05	2.10 ± 0.78	0
1.28	14.80 ± 0.89	0.60 ± 0.51	1	2.24	18.20 ± 1.06	2.12 ± 0.78	0
1.30	15.08 ± 0.90	0.30 ± 0.52	0	2.26	17.84 ± 1.04	2.72 ± 0.93	1
1.32	15.64 ± 0.94	0.30 ± 0.52	0	2.28	18.45 ± 1.07	2.74 ± 0.93	1
1.34	15.49 ± 0.93	0.20 ± 0.51	0	2.30	18.05 ± 1.05	2.04 ± 0.63	1
1.36	15.50 ± 0.93	0.00 ± 0.49	2	2.32	18.34 ± 1.06	1.72 ± 0.61	1
1.38	15.48 ± 0.93	0.60 ± 0.51	1	2.34	18.49 ± 1.07	0.77 ± 0.56	0
1.40	15.57 ± 0.93	1.00 ± 0.55	1	2.36	18.18 ± 1.05	1.15 ± 0.59	0
1.42	15.52 ± 0.93	0.40 ± 0.53	0	2.38	18.40 ± 1.06	1.15 ± 0.59	1
1.44	15.64 ± 0.94	0.60 ± 0.51	0	2.40	19.01 ± 1.09	2.05 ± 0.66	2
1.46	15.84 ± 0.95	0.70 ± 0.52	0	2.42	18.79 ± 1.07	2.50 ± 0.70	2
1.48	15.80 ± 0.95	1.50 ± 0.74	0	2.44	18.69 ± 1.06	2.30 ± 0.68	2
1.50	15.63 ± 0.94	1.10 ± 0.56	1	2.46	18.69 ± 1.06	3.10 ± 0.71	2
1.52	15.75 ± 0.95	1.15 ± 0.56	1	2.48	18.79 ± 1.06	3.40 ± 0.86	1
1.54	15.69 ± 0.94	0.60 ± 0.54	1	2.50	18.73 ± 1.05	2.40 ± 0.66	1
1.56	16.25 ± 0.98	1.15 ± 0.55	0	2.52	19.12 ± 1.07	2.05 ± 0.63	1
1.58	16.15 ± 0.97	0.90 ± 0.53	0	2.54	21.35 ± 1.18	3.75 ± 1.08	2
1.60	15.84 ± 0.95	0.85 ± 0.53	0	2.56	21.30 ± 1.17	3.05 ± 0.95	1
1.62	15.61 ± 0.94	0.45 ± 0.53	0	2.58	21.96 ± 1.18	3.35 ± 0.97	1
1.64	15.60 ± 0.94	0.55 ± 0.54	0	2.60	22.52 ± 1.19	2.25 ± 0.79	0
1.66	15.11 ± 0.91	0.55 ± 0.54	0	2.62	22.94 ± 1.18	0.80 ± 0.56	0
1.68	14.50 ± 0.87	0.50 ± 0.54	0				

Table 5: Signal efficiency (ϵ), the number of expected background events (N_{bkg}), and the number of observed events (N_{obs}) for $B^0 \rightarrow A'A' \rightarrow \mu^+\mu^-\pi^+\pi^-$ mode.

$m_{A'}$ (GeV/ c^2)	ϵ (%)	N_{bkg}	N_{obs}	$m_{A'}$ (GeV/ c^2)	ϵ (%)	N_{bkg}	N_{obs}
0.28	20.99 ± 1.25	0.00 ± 0.49	0	1.70	8.68 ± 0.52	0.00 ± 0.49	0
0.29	20.42 ± 1.22	0.00 ± 0.49	0	1.72	8.02 ± 0.48	0.00 ± 0.49	0
0.30	19.85 ± 1.18	0.50 ± 0.50	0	1.74	8.67 ± 0.52	0.00 ± 0.49	0
0.31	19.41 ± 1.15	0.50 ± 0.50	0	1.76	5.68 ± 0.34	0.10 ± 0.50	0
0.32	18.97 ± 1.12	0.00 ± 0.49	0	1.78	4.48 ± 0.28	0.10 ± 0.50	0
0.33	18.45 ± 1.09	0.50 ± 0.50	0	1.80	8.58 ± 0.54	0.00 ± 0.49	0
0.34	17.93 ± 1.06	0.00 ± 0.49	0	1.82	11.76 ± 0.72	0.20 ± 0.51	1
0.35	17.67 ± 1.04	0.00 ± 0.49	0	1.84	11.40 ± 0.71	0.10 ± 0.50	0
0.36	17.42 ± 1.02	0.00 ± 0.49	0	1.88	6.46 ± 0.40	0.10 ± 0.50	0
0.37	16.87 ± 1.00	0.00 ± 0.49	0	1.90	12.91 ± 0.80	0.00 ± 0.49	0
0.38	16.33 ± 0.97	0.00 ± 0.49	0	1.92	13.31 ± 0.82	0.00 ± 0.49	0
0.39	15.81 ± 0.94	0.00 ± 0.49	0	1.94	13.75 ± 0.85	0.10 ± 0.50	0
0.40	15.30 ± 0.91	0.00 ± 0.49	0	1.96	14.01 ± 0.86	0.00 ± 0.49	0
0.41	14.98 ± 0.90	0.00 ± 0.49	0	1.98	14.22 ± 0.88	0.20 ± 0.51	0
0.42	14.66 ± 0.88	0.00 ± 0.49	0	2.00	14.62 ± 0.90	0.10 ± 0.50	0
0.43	14.31 ± 0.86	0.00 ± 0.49	0	2.02	14.84 ± 0.91	0.20 ± 0.51	0
0.44	13.95 ± 0.84	0.00 ± 0.49	0	2.04	15.19 ± 0.92	0.10 ± 0.50	0
1.10	9.87 ± 0.56	0.50 ± 0.50	0	2.06	15.53 ± 0.94	0.10 ± 0.50	0
1.12	9.88 ± 0.56	0.50 ± 0.50	0	2.08	15.96 ± 0.96	0.10 ± 0.50	0

1.14	9.88 ± 0.56	0.10 ± 0.50	0	2.10	16.28 ± 0.98	0.27 ± 0.51	0
1.16	9.82 ± 0.56	0.00 ± 0.49	0	2.12	16.46 ± 0.98	0.22 ± 0.51	0
1.18	9.77 ± 0.55	0.00 ± 0.49	0	2.14	16.84 ± 1.00	0.20 ± 0.51	0
1.20	9.87 ± 0.56	0.00 ± 0.49	0	2.16	17.15 ± 1.01	0.10 ± 0.50	0
1.22	9.76 ± 0.56	0.50 ± 0.50	0	2.18	17.52 ± 1.03	0.10 ± 0.50	1
1.24	9.96 ± 0.57	0.00 ± 0.49	0	2.20	17.76 ± 1.04	0.00 ± 0.49	0
1.26	9.93 ± 0.57	0.10 ± 0.50	0	2.22	18.08 ± 1.05	0.10 ± 0.50	0
1.28	9.73 ± 0.56	0.50 ± 0.50	1	2.24	18.66 ± 1.08	0.60 ± 0.51	0
1.30	9.81 ± 0.56	0.00 ± 0.49	0	2.26	18.95 ± 1.09	0.30 ± 0.52	0
1.32	9.86 ± 0.57	0.10 ± 0.50	0	2.28	19.26 ± 1.10	0.00 ± 0.49	0
1.34	9.77 ± 0.56	0.10 ± 0.50	0	2.30	19.74 ± 1.12	0.20 ± 0.51	0
1.36	9.76 ± 0.56	0.50 ± 0.50	0	2.32	19.99 ± 1.14	0.30 ± 0.52	0
1.38	9.58 ± 0.55	0.00 ± 0.49	0	2.34	20.31 ± 1.15	0.10 ± 0.50	0
1.40	9.76 ± 0.57	0.00 ± 0.49	0	2.36	20.66 ± 1.17	0.00 ± 0.49	1
1.42	9.71 ± 0.57	0.10 ± 0.50	0	2.38	20.98 ± 1.18	0.12 ± 0.50	1
1.44	9.75 ± 0.57	0.10 ± 0.50	0	2.40	20.87 ± 1.17	0.72 ± 0.52	0
1.46	9.76 ± 0.57	0.10 ± 0.50	0	2.42	21.57 ± 1.21	1.30 ± 0.73	0
1.48	9.65 ± 0.57	0.00 ± 0.49	0	2.44	22.02 ± 1.24	0.40 ± 0.53	0
1.50	9.94 ± 0.59	0.00 ± 0.49	0	2.46	22.41 ± 1.26	0.70 ± 0.52	0
1.52	9.83 ± 0.58	0.00 ± 0.49	0	2.48	22.53 ± 1.27	0.50 ± 0.50	0
1.54	9.85 ± 0.59	0.00 ± 0.49	0	2.50	23.08 ± 1.30	0.50 ± 0.50	0
1.56	9.92 ± 0.59	0.00 ± 0.49	0	2.52	23.45 ± 1.32	0.62 ± 0.51	0
1.58	9.65 ± 0.58	0.00 ± 0.49	0	2.54	23.91 ± 1.35	0.32 ± 0.52	0
1.60	9.44 ± 0.57	0.00 ± 0.49	0	2.56	24.17 ± 1.36	0.42 ± 0.53	1
1.62	9.41 ± 0.56	0.00 ± 0.49	0	2.58	24.50 ± 1.38	0.52 ± 0.54	1
1.64	9.07 ± 0.55	0.00 ± 0.49	0	2.60	25.34 ± 1.43	1.52 ± 0.74	0
1.66	8.93 ± 0.54	0.00 ± 0.49	0	2.62	25.74 ± 1.45	1.52 ± 0.87	0
1.68	8.86 ± 0.53	0.00 ± 0.49	0				

Table 6: Signal efficiency (ϵ), the number of expected background events (N_{bkg}), and the number of observed events (N_{obs}) for a combined $B^0 \rightarrow A'A'$.

$m_{A'}$ (GeV/ c^2)	ϵ (%)	N_{bkg}	N_{obs}	$m_{A'}$ (GeV/ c^2)	ϵ (%)	N_{bkg}	N_{obs}
0.01	14.56 ± 1.34	0.33 ± 0.24	1	0.94	3.63 ± 0.08	0.10 ± 0.30	0
0.02	14.82 ± 1.36	0.83 ± 0.37	2	0.95	3.84 ± 0.09	0.10 ± 0.30	0
0.03	14.72 ± 1.35	0.50 ± 0.29	1	0.96	3.91 ± 0.09	0.00 ± 0.29	0
0.04	14.62 ± 1.33	0.00 ± 0.17	1	0.97	4.19 ± 0.10	0.00 ± 0.29	0
0.05	14.51 ± 1.32	0.00 ± 0.17	1	0.98	4.03 ± 0.10	0.00 ± 0.29	0
0.06	14.40 ± 1.31	0.00 ± 0.17	0	0.99	4.28 ± 0.11	0.00 ± 0.29	0
0.07	14.24 ± 1.30	0.00 ± 0.17	1	1.00	3.53 ± 0.09	0.00 ± 0.29	0
0.08	14.08 ± 1.28	0.00 ± 0.17	1	1.01	1.98 ± 0.05	0.00 ± 0.29	0
0.09	13.86 ± 1.26	0.00 ± 0.17	0	1.02	0.02 ± 0.00	0.00 ± 0.29	0
0.10	13.64 ± 1.24	0.00 ± 0.17	0	1.03	1.24 ± 0.03	0.00 ± 0.29	0
0.11	13.65 ± 1.24	0.00 ± 0.17	0	1.04	2.73 ± 0.07	0.00 ± 0.29	0
0.12	13.66 ± 1.24	0.00 ± 0.17	0	1.05	3.42 ± 0.09	0.00 ± 0.29	0
0.13	13.76 ± 1.25	0.00 ± 0.17	0	1.06	3.84 ± 0.11	0.00 ± 0.29	0

0.14	13.85 ± 1.26	0.00 ± 0.17	0	1.07	3.83 ± 0.11	0.00 ± 0.29	0
0.15	13.71 ± 1.25	0.00 ± 0.17	0	1.08	3.94 ± 0.12	0.00 ± 0.29	0
0.16	13.57 ± 1.24	0.00 ± 0.17	0	1.09	4.19 ± 0.13	0.00 ± 0.29	0
0.17	13.47 ± 1.23	0.00 ± 0.17	0	1.10	7.64 ± 0.25	0.80 ± 0.78	0
0.18	13.37 ± 1.22	0.00 ± 0.17	0	1.12	7.30 ± 0.25	0.74 ± 0.77	0
0.19	13.31 ± 1.21	0.00 ± 0.17	0	1.14	6.85 ± 0.24	0.74 ± 0.77	0
0.20	13.25 ± 1.21	0.00 ± 0.17	0	1.16	6.49 ± 0.23	0.62 ± 0.76	0
0.21	13.22 ± 1.20	0.00 ± 0.17	0	1.18	6.38 ± 0.23	0.85 ± 0.78	1
0.22	19.39 ± 1.06	0.00 ± 0.29	0	1.20	6.08 ± 0.23	0.25 ± 0.76	1
0.23	19.91 ± 1.00	0.00 ± 0.29	0	1.22	5.53 ± 0.22	0.70 ± 0.77	0
0.24	19.50 ± 0.95	0.00 ± 0.29	0	1.24	5.75 ± 0.21	0.25 ± 0.76	0
0.25	18.39 ± 0.88	0.00 ± 0.29	0	1.26	5.27 ± 0.21	0.85 ± 0.78	1
0.26	17.04 ± 0.80	0.00 ± 0.29	0	1.28	4.54 ± 0.19	1.10 ± 0.77	2
0.27	16.12 ± 0.76	0.00 ± 0.29	0	1.30	4.68 ± 0.19	0.30 ± 0.77	0
0.28	15.14 ± 0.71	0.00 ± 0.75	0	1.32	4.53 ± 0.19	0.40 ± 0.77	0
0.29	14.62 ± 0.68	0.50 ± 0.76	0	1.34	4.18 ± 0.17	0.40 ± 0.77	0
0.30	14.10 ± 0.64	0.50 ± 0.76	0	1.36	3.68 ± 0.16	0.60 ± 0.76	2
0.31	13.84 ± 0.62	0.50 ± 0.76	0	1.38	3.48 ± 0.15	0.80 ± 0.77	1
0.32	13.58 ± 0.60	0.00 ± 0.75	0	1.40	3.03 ± 0.14	1.10 ± 0.79	1
0.33	13.37 ± 0.58	0.50 ± 0.76	0	1.42	3.32 ± 0.15	0.60 ± 0.79	0
0.34	13.16 ± 0.57	0.00 ± 0.75	0	1.44	3.51 ± 0.16	0.70 ± 0.77	0
0.35	12.97 ± 0.55	0.00 ± 0.75	0	1.46	3.00 ± 0.14	0.80 ± 0.77	0
0.36	12.80 ± 0.53	0.00 ± 0.75	0	1.48	2.48 ± 0.12	1.50 ± 0.93	0
0.37	12.65 ± 0.52	0.00 ± 0.75	0	1.50	2.27 ± 0.11	1.10 ± 0.79	1
0.38	12.45 ± 0.50	0.00 ± 0.75	0	1.52	2.31 ± 0.11	1.15 ± 0.80	1
0.39	12.69 ± 0.51	0.50 ± 0.76	0	1.54	2.27 ± 0.11	0.60 ± 0.78	1
0.40	12.54 ± 0.49	0.50 ± 0.76	0	1.56	2.18 ± 0.11	1.15 ± 0.79	0
0.41	12.63 ± 0.48	0.50 ± 0.76	0	1.58	2.20 ± 0.11	0.90 ± 0.78	0
0.42	12.89 ± 0.48	0.00 ± 0.75	0	1.60	2.12 ± 0.10	0.85 ± 0.78	0
0.43	12.50 ± 0.46	0.00 ± 0.75	0	1.62	2.14 ± 0.10	0.45 ± 0.78	0
0.44	11.85 ± 0.44	0.50 ± 0.76	0	1.64	1.84 ± 0.09	0.55 ± 0.78	0
0.45	8.27 ± 0.29	0.00 ± 0.29	0	1.66	1.85 ± 0.09	0.55 ± 0.78	0
0.46	8.34 ± 0.29	0.00 ± 0.29	0	1.68	1.95 ± 0.10	0.50 ± 0.78	0
0.47	7.83 ± 0.26	0.00 ± 0.29	0	1.70	1.98 ± 0.10	0.40 ± 0.77	0
0.48	7.42 ± 0.24	0.00 ± 0.29	0	1.72	2.06 ± 0.10	0.30 ± 0.77	0
0.49	7.18 ± 0.23	0.00 ± 0.29	0	1.74	2.11 ± 0.10	0.20 ± 0.76	0
0.50	6.93 ± 0.21	0.00 ± 0.29	0	1.76	1.90 ± 0.09	0.40 ± 0.77	0
0.51	6.54 ± 0.20	0.00 ± 0.29	0	1.78	2.00 ± 0.10	0.50 ± 0.78	0
0.52	6.49 ± 0.19	0.00 ± 0.29	0	1.80	2.30 ± 0.11	0.40 ± 0.77	0
0.53	5.90 ± 0.17	0.00 ± 0.29	0	1.82	2.52 ± 0.12	0.80 ± 0.80	1
0.54	5.58 ± 0.15	0.00 ± 0.29	0	1.84	2.41 ± 0.11	1.00 ± 0.79	0
0.55	5.36 ± 0.14	0.00 ± 0.29	0	1.86	2.87 ± 0.14	0.80 ± 0.78	0
0.56	5.09 ± 0.13	0.00 ± 0.29	0	1.88	2.98 ± 0.14	1.40 ± 0.93	0
0.57	4.79 ± 0.11	0.00 ± 0.29	0	1.90	2.96 ± 0.15	0.60 ± 0.79	0
0.58	4.52 ± 0.10	0.00 ± 0.29	0	1.92	2.95 ± 0.15	0.95 ± 0.81	0
0.59	4.10 ± 0.08	0.10 ± 0.30	0	1.94	2.91 ± 0.15	1.25 ± 0.82	0
0.60	3.74 ± 0.07	0.10 ± 0.30	0	1.96	2.54 ± 0.13	1.07 ± 0.81	0
0.61	3.37 ± 0.06	0.10 ± 0.30	0	1.98	2.53 ± 0.13	1.97 ± 0.84	0
0.62	3.14 ± 0.06	0.10 ± 0.30	0	2.00	2.88 ± 0.14	1.67 ± 0.83	0

0.63	2.69 ± 0.04	0.10 ± 0.30	0	2.02	2.89 ± 0.14	1.94 ± 0.84	0
0.64	2.70 ± 0.04	0.10 ± 0.30	0	2.04	2.91 ± 0.14	1.92 ± 0.84	1
0.65	2.04 ± 0.03	0.00 ± 0.29	0	2.06	2.94 ± 0.14	1.67 ± 0.85	1
0.66	1.80 ± 0.03	0.00 ± 0.29	0	2.08	2.96 ± 0.15	1.20 ± 0.82	1
0.67	1.59 ± 0.02	0.00 ± 0.29	0	2.10	3.00 ± 0.15	1.17 ± 0.82	0
0.68	1.19 ± 0.01	0.00 ± 0.29	0	2.12	3.01 ± 0.15	2.17 ± 0.86	2
0.69	1.04 ± 0.01	0.00 ± 0.29	0	2.14	3.07 ± 0.15	2.00 ± 0.85	2
0.70	0.86 ± 0.01	0.00 ± 0.29	0	2.16	3.11 ± 0.15	2.30 ± 0.87	2
0.71	0.70 ± 0.01	0.00 ± 0.29	0	2.18	3.15 ± 0.15	2.00 ± 0.87	1
0.72	0.57 ± 0.00	0.00 ± 0.29	0	2.20	3.20 ± 0.15	1.60 ± 0.85	0
0.73	0.48 ± 0.00	0.00 ± 0.29	0	2.22	3.29 ± 0.16	2.50 ± 0.98	0
0.74	0.31 ± 0.00	0.00 ± 0.29	0	2.24	3.38 ± 0.16	3.02 ± 0.99	0
0.75	0.36 ± 0.00	0.00 ± 0.29	0	2.26	3.47 ± 0.16	3.22 ± 1.11	1
0.76	0.33 ± 0.00	0.00 ± 0.29	0	2.28	3.56 ± 0.17	2.94 ± 1.10	1
0.77	0.28 ± 0.00	0.00 ± 0.29	0	2.30	3.64 ± 0.17	2.34 ± 0.87	1
0.78	0.11 ± 0.00	0.00 ± 0.29	0	2.32	3.73 ± 0.17	2.12 ± 0.85	1
0.79	0.31 ± 0.00	0.00 ± 0.29	0	2.34	3.82 ± 0.18	1.07 ± 0.81	0
0.80	0.50 ± 0.00	0.00 ± 0.29	0	2.36	3.92 ± 0.18	1.35 ± 0.83	1
0.81	0.65 ± 0.01	0.00 ± 0.29	0	2.38	4.01 ± 0.18	1.47 ± 0.84	2
0.82	0.81 ± 0.01	0.00 ± 0.29	0	2.40	4.11 ± 0.19	2.97 ± 0.90	2
0.83	0.95 ± 0.01	0.00 ± 0.29	0	2.42	4.20 ± 0.19	4.00 ± 1.06	2
0.84	1.19 ± 0.01	0.00 ± 0.29	0	2.44	4.28 ± 0.19	2.90 ± 0.92	2
0.85	1.50 ± 0.02	0.00 ± 0.29	0	2.46	4.38 ± 0.20	4.00 ± 0.94	2
0.86	1.48 ± 0.02	0.00 ± 0.29	0	2.48	4.49 ± 0.20	4.10 ± 1.05	1
0.87	1.98 ± 0.03	0.00 ± 0.29	0	2.50	4.59 ± 0.21	3.10 ± 0.89	1
0.88	2.17 ± 0.03	0.00 ± 0.29	0	2.52	4.61 ± 0.20	2.67 ± 0.86	1
0.89	2.57 ± 0.04	0.00 ± 0.29	0	2.54	4.62 ± 0.20	4.07 ± 1.23	2
0.90	2.76 ± 0.05	0.00 ± 0.29	0	2.56	4.65 ± 0.20	3.47 ± 1.12	2
0.91	3.06 ± 0.06	0.00 ± 0.29	0	2.58	4.69 ± 0.20	3.97 ± 1.15	2
0.92	3.14 ± 0.06	0.10 ± 0.30	0	2.60	4.74 ± 0.20	3.87 ± 1.12	0
0.93	3.44 ± 0.07	0.10 ± 0.30	0	2.62	5.00 ± 0.21	2.42 ± 1.08	0

2 Upper limits of branching fraction

The following table presents upper limits at 90% confidence level for three kinds of branching fraction: (a) $\text{B.F.}(B^0 \rightarrow A'A') \equiv \mathcal{B}$, (b) $\text{B.F.}(B^0 \rightarrow A'A') \times \text{B.F.}(A' \rightarrow e^+e^-)^2 \equiv \mathcal{B}_{ee}$, (c) $\text{B.F.}(B^0 \rightarrow A'A') \times \text{B.F.}(A' \rightarrow \mu^+\mu^-)^2 \equiv \mathcal{B}_{\mu\mu}$. The dark photon is scanned in $0.01 - 2.62 \text{ GeV}/c^2$ mass range with $10 \text{ MeV}/c^2$ ($0.01 - 1.10 \text{ GeV}/c^2$) and $20 \text{ MeV}/c^2$ ($1.10 - 2.62 \text{ GeV}/c^2$) intervals. The upper limits are calculated using the POLE program [4] which is based on the Feldman-Cousins unified approach [5].

Table 7: Upper limits of branching fractions at 90% confidence level.

$m_{A'}$ (GeV/c^2)	\mathcal{B} (10^{-8})	\mathcal{B}_{ee} (10^{-8})	$\mathcal{B}_{\mu\mu}$ (10^{-8})	$m_{A'}$ (GeV/c^2)	\mathcal{B} (10^{-8})	\mathcal{B}_{ee} (10^{-8})	$\mathcal{B}_{\mu\mu}$ (10^{-8})
0.01	3.64	3.64	-	0.94	8.22	2.83	4.80
0.02	4.55	4.55	-	0.95	7.78	2.82	4.81
0.03	3.47	3.47	-	0.96	7.79	2.81	4.81

0.04	3.85	3.85	-	0.97	7.25	2.81	4.83
0.05	3.88	3.88	-	0.98	7.54	2.82	4.84
0.06	2.21	2.21	-	0.99	7.10	2.82	4.88
0.07	3.95	3.95	-	1.00	8.63	2.83	4.92
0.08	4.00	4.00	-	1.01	15.4	2.83	4.94
0.09	2.30	2.30	-	1.02	1763	2.83	4.94
0.10	2.34	2.34	-	1.03	24.5	2.83	4.95
0.11	2.33	2.33	-	1.04	11.1	2.84	4.96
0.12	2.33	2.33	-	1.05	8.89	2.84	4.99
0.13	2.32	2.32	-	1.06	7.91	2.85	5.03
0.14	2.30	2.30	-	1.07	7.95	2.85	5.05
0.15	2.32	2.32	-	1.08	7.72	2.85	5.07
0.16	2.35	2.35	-	1.09	7.26	2.86	5.07
0.17	2.37	2.37	-	1.10	3.30	2.87	5.06
0.18	2.38	2.38	-	1.12	3.51	2.87	5.06
0.19	2.39	2.39	-	1.14	3.74	2.88	5.02
0.20	2.41	2.41	-	1.16	4.05	2.88	5.02
0.21	2.41	2.41	-	1.18	7.21	2.88	5.02
0.22	1.58	2.42	0.92	1.20	8.29	2.88	5.00
0.23	1.53	2.44	1.01	1.22	4.68	2.87	4.97
0.24	1.57	2.46	1.13	1.24	4.89	2.88	4.95
0.25	1.66	2.46	1.31	1.26	8.74	2.86	4.99
0.26	1.79	2.46	1.57	1.28	14.0	2.86	4.95
0.27	1.89	2.46	1.76	1.30	5.95	2.84	4.96
0.28	1.94	2.47	2.02	1.32	6.03	2.83	4.95
0.29	1.84	2.48	2.19	1.34	6.54	2.83	4.93
0.30	1.91	2.49	2.39	1.36	18.6	2.81	4.95
0.31	1.95	2.50	2.52	1.38	13.3	2.79	4.90
0.32	2.16	2.51	2.66	1.40	14.5	2.78	4.93
0.33	2.01	2.52	2.77	1.42	7.92	2.75	4.91
0.34	2.23	2.53	2.89	1.44	7.38	2.76	4.91
0.35	2.26	2.54	3.04	1.46	8.41	2.73	4.92
0.36	2.29	2.55	3.21	1.48	8.19	2.72	4.90
0.37	2.32	2.56	3.24	1.50	19.3	2.71	4.94
0.38	2.36	2.56	3.27	1.52	18.7	2.69	4.90
0.39	2.12	2.57	3.36	1.54	21.1	2.67	4.90
0.40	2.15	2.58	3.44	1.56	10.6	2.64	4.89
0.41	2.13	2.59	3.51	1.58	11.2	2.64	4.84
0.42	2.28	2.60	3.58	1.60	11.8	2.63	4.81
0.43	2.35	2.61	3.64	1.62	12.7	2.63	4.83
0.44	2.27	2.61	3.71	1.64	14.4	2.62	4.79
0.45	3.69	2.63	3.75	1.66	14.3	2.61	4.73
0.46	3.66	2.65	3.79	1.68	13.7	2.59	4.70
0.47	3.90	2.67	3.83	1.70	13.8	2.58	4.70
0.48	4.11	2.69	3.88	1.72	13.6	2.56	4.62
0.49	4.25	2.71	3.92	1.74	13.5	2.56	4.56
0.50	4.39	2.73	3.96	1.76	14.4	2.55	4.53
0.51	4.65	2.76	3.99	1.78	13.4	2.53	4.48
0.52	4.69	2.79	4.01	1.80	11.9	2.51	4.42

0.53	5.15	2.81	4.05	1.82	18.4	2.49	4.34
0.54	5.44	2.83	4.09	1.84	9.98	2.47	4.39
0.55	5.67	2.85	4.11	1.86	8.77	2.47	4.21
0.56	5.97	2.87	4.13	1.88	6.98	2.45	4.13
0.57	6.34	2.87	4.15	1.90	8.86	2.38	4.03
0.58	6.72	2.87	4.18	1.92	8.18	2.37	3.94
0.59	7.28	2.80	4.19	1.94	7.66	2.35	3.86
0.60	7.99	2.81	4.20	1.96	9.18	2.34	3.76
0.61	8.85	2.82	4.22	1.98	7.02	2.22	3.65
0.62	9.52	2.84	4.25	2.00	6.80	2.21	3.62
0.63	11.1	2.84	4.28	2.02	6.23	2.19	3.48
0.64	11.1	2.84	4.31	2.04	11.9	2.25	3.37
0.65	14.9	2.92	4.32	2.06	12.8	2.23	3.26
0.66	16.9	2.92	4.32	2.08	14.4	2.22	3.16
0.67	19.1	2.92	4.34	2.10	7.61	2.21	3.03
0.68	25.5	2.92	4.36	2.12	17.1	2.20	2.93
0.69	29.2	2.91	4.38	2.14	17.7	2.14	2.80
0.70	35.2	2.91	4.40	2.16	16.0	2.13	2.70
0.71	43.5	2.90	4.42	2.18	10.8	2.12	2.59
0.72	53.2	2.89	4.44	2.20	6.25	2.09	2.48
0.73	62.9	2.88	4.46	2.22	4.34	2.06	2.36
0.74	97.8	2.87	4.49	2.24	3.39	2.04	2.25
0.75	84.6	2.85	4.49	2.26	7.99	2.01	2.15
0.76	93.3	2.83	4.49	2.28	8.47	2.06	2.07
0.77	111	2.81	4.52	2.30	8.38	2.08	1.99
0.78	288	2.80	4.54	2.32	8.76	2.05	1.91
0.79	98.4	2.80	4.54	2.34	6.14	1.97	1.84
0.80	61.3	2.80	4.54	2.36	10.4	1.88	1.78
0.81	46.5	2.79	4.56	2.38	14.9	1.85	1.71
0.82	37.6	2.79	4.59	2.40	10.2	1.83	1.65
0.83	32.1	2.78	4.61	2.42	8.61	1.79	1.61
0.84	25.6	2.77	4.63	2.44	10.1	1.79	1.55
0.85	20.3	2.77	4.63	2.46	7.06	1.73	1.51
0.86	20.6	2.76	4.63	2.48	4.69	1.70	1.46
0.87	15.4	2.77	4.67	2.50	5.20	1.66	1.42
0.88	14.0	2.78	4.72	2.52	5.96	1.71	1.37
0.89	11.8	2.78	4.71	2.54	7.71	1.69	1.33
0.90	11.0	2.78	4.69	2.56	8.89	1.62	1.28
0.91	9.94	2.78	4.71	2.58	7.76	1.57	1.23
0.92	9.52	2.78	4.73	2.60	2.31	1.50	1.18
0.93	8.68	2.80	4.76	2.62	2.88	1.47	1.15

References

- [1] P. A. Zyla *et al.* (Particle Data Group), *The Review of Particle Physics*, to be published in PTEP **2020** (2020) 083C01.
- [2] B. Batell, M. Pospelov and A. Ritz, *Probing a Secluded $U(1)$ at B -factories*, Phys. Rev. D **79** (2009) 115008 [arXiv:0903.0363].

- [3] J. P. Lees *et al.* (BaBar Collaboration), *Search for Low-Mass Dark-Sector Higgs Bosons*, Phys. Rev. Lett. **108** (2012) 211801 [arXiv:1202.1313].
- [4] J. Conrad, O. Botner, A. Hallgren and C. Perez de los Heros, *Including systematic uncertainties in confidence interval construction for Poisson statistics*, Phys. Rev. D **67** (2003) 012002 [arXiv:hep-ex/0202013].
- [5] G. J. Feldman and R. D. Cousins, *A Unified approach to the classical statistical analysis of small signals*, Phys. Rev. D **57** (1998) 3873 [arXiv:physics/9711021].